AEDC-TR-71-23

Copy 1

FINAL RESULTS OF ON-LINE MASS SPECTROMETRIC ANALYSIS OF NONEQUILIBRIUM AIRFLOWS

W. N. MacDermott and R. E. Dix

ARO, Inc.

February 1971

This document has been approved for public release and sale; its distribution is unlimited.

PROPULSION WIND TUNNEL FACILITY
ARNOLD ENGINEERING DEVELOPMENT CENTER
AIR FORCE SYSTEMS COMMAND
ARNOLD AIR FORCE STATION, TENNESSEE

NOTICES

FINAL RESULTS OF ON-LINE MASS SPECTROMETRIC ANALYSIS OF NONEQUILIBRIUM AIRFLOWS

W. N. MacDermott and R. E. Dix
ARO, Inc.

FOREWORD

The research report herein was sponsored by Arnold Engineering Development Center (AEDC), Air Force Systems Command (AFSC), Arnold Air Force Station, Tennessee, under Program Element 65701, Project 4344, Task 02.

The results of the research were obtained by ARO, Inc. (a subsidiary of Sverdrup & Parcel and Associates, Inc.), contract operator of AEDC, AFSC, under Contract F40600-71-C-0002. The research was conducted from July 1, 1969, to June 30, 1970, under ARO Project No. PL3012, and the manuscript was submitted for publication on October 5, 1970.

This technical report has been reviewed and is approved.

Vincent A. Rocco
First Lieutenant, USAF
Research and Development
Division
Directorate of Technology

Harry L. Maynard
Colonel, USAF
Director of Technology

ABSTRACT

Comprehensive determinations of nonequilibrium airflow compositions were made in frozen expansions of arc-heated air in a low-density wind tunnel nozzle. Reservoir conditions included pressures of from 3.7 to 20.8 atm and temperatures of from 2120 to 5380°K. The experimentally determined compositions were correlated with the reservoir entropy. At low entropy, the concentrations of molecular species were generally in close agreement with predictions based on finite rate expansion calculations, but at high entropy, where nonequilibrium effects are large, considerable deviations from the predictions were observed. The molecular oxygen content was determined to be 7 percent greater than expected. The atomic oxygen concentration was determined to be consistently less than the theoretical prediction for all values of entropy, by as much as 9 percent of the total sample in the worst case. The experimental data were consistent, however, with theoretical predictions based on oxygen recombination rates 100 times the generally accepted values. Compositions were determined with a mass spectrometric sampling probe. The notable features of the probe included a liquid-hydrogen cryopump and a quadrupole mass spectrometer. The mass spectrometer exhibited large uncertainties when attempts were made to determine absolute concentrations, particularly in a contaminated system. For determination of relative compositions in a clean system, repeatabilities of a few percent were demonstrated.

CONTENTS

APPENDIX
ILLUSTRATIONS

NOMENCLATURE

$c_{i,j}$	Absolute sensitivity of the mass spectrometer to ions of m/e = i derived from "parent" particles of mass j
F_i	Factor expressing the influence of the mass spectrometer itself upon particles of m/e = i
I_i	Output current of the mass spectrometer for m/e = i
$I_{i,j}$	Output current for m/e = i derived from particles of mass j
i_e	Current in electron beam of the ionizer
K_c	Equilibrium constant
k_b	Reverse reaction rate constant

k_f	Forward reaction rate constant
L_{eff}	Effective length of the electron beam in the ionizer
M_i	Molecular weight
m/e	Mass-to-charge ratio
n_i	Number of particles per unit volume for particles of mass i
p_{t_1}	Stagnation pressure in the reservoir
S/R	Dimensionless entropy parameter, $\frac{\text{reservoir entropy}}{\text{specific gas constant}}$
T	Absolute temperature of gas
T_{t_1}	Stagnation temperature in the reservoir
v_{ee}	Electron energy, v
$\bar{v}_i$	Mean thermal velocity of particles of m/e = i
η_f	Constant for a given molecule
θ_D	Characteristic temperature for dissociation
$\sigma_{i,j}$	Ionization cross section for production of particles of m/e = i by collision of electrons with particles of mass j

SECTION I
INTRODUCTION

Rapid expansion of high enthalpy gases in converging-diverging nozzles generally produces some degree of chemical nonequilibrium. Flow theories exist that relate the characteristic rates of chemical reactions and vibrational energy exchanges to the rates of change of thermodynamic parameters. Verification of such theories is quite difficult because of experimental difficulties in determining the state of a gas that is not in equilibrium. In general, there is a correspondence between the number of independent measurements required and the number of degrees of freedom in which the gas is not in equilibrium. When chemical nonequilibrium exists in a complex gas, such as air, the number and quality of measurements required to completely define the state of the gas are frequently greater than technology can provide.

For a number of years, limited verifications were provided by a small number of measurements representing more-or-less conventional wind tunnel techniques, i.e., pitot and static pressures and mass flux measurements (Refs. 1 through 3). The development of the electron beam probe as a wind tunnel diagnostic tool expanded the scope of verification of finite rate expansion theories by adding static temperature, vibrational temperature, and static density to the group of available measurements (Refs. 4 through 6). In Ref. 7, results were reported of a comprehensive application of the electron beam to demonstrate a detailed correlation of finite rate effects with the reservoir entropy in an arc-heated airflow. The correlation was demonstrated systematically through a graduated succession of nonequilibrium states from a case of small perturbation of the equilibrium state to an extreme case with order-of-magnitude effects on the thermodynamic parameters. Across the entire range, the experimental measurements appeared to verify the finite rate theory. A minor exception was the vibrational temperature of nitrogen molecules, which appeared to show a faster vibrational adjustment than predicted from shock tube experiments. Similar behavior of vibrational adjustment had previously been observed in other nozzle expansions (Refs. 8 through 10).

Because the thermodynamic calibrations of finite rate expansions have been basically incomplete, there has been considerable interest in supplementing them with chemical measurements. Chemical calibrations of nonequilibrium flows have proved to be even more difficult than thermodynamic calibrations. At least three different techniques have been applied to this problem: optical spectroscopy, catalytic probes, and mass spectrometry.

Optical techniques have been used in shock tube facilities to obtain basic chemical rate data, but there has been little, if any, application of such techniques to the determination of detailed nonequilibrium composition in continuous flow facilities.

The catalytic probe technique has been under development for a number of years. It is a very complicated technique requiring critical control of the chemical condition of the catalytic surface. A recent report (Ref. 11) presented a limited amount of data obtained with the catalytic probe. The data indicated that the atomic oxygen fraction in a shock tunnel expansion of air was less than that predicted by a finite rate calculation, an indication in agreement with results of this report.

The potential usefulness of mass spectrometry in nonequilibrium chemical research was recognized a number of years ago, and the technique was applied in short-duration shock tube experiments (Ref. 12). Initial attempts to utilize the technique in continuous flow facilities were not notably successful in a quantitative sense (Refs. 13 and 14) but indicated that the main problem lay in the aerodynamics of obtaining an undisturbed sample of the flow. The requirements for sampling in place were recognized to be a mass spectrometer compact enough to fit within a small-sized sampling probe and a pumping system of sufficient capacity to maintain the internal pressure of the probe at 10^{-4} torr or less. These requirements were met by a quadrupole mass spectrometer and a liquid-hydrogen cryopump. Basic development and feasibility tests with such a probe at PWT-AEDC were reported in Ref. 15. Uncalibrated determinations of molecular nitrogen, molecular oxygen, and nitric oxide concentrations in an arc-heated airflow were observed to be in reasonable agreement with theory for a single modest operating condition, but the lower limit of detectability was inadequate for accurate determination of atomic oxygen or atomic nitrogen concentrations.

Since the report disclosing basic feasibility was printed, the performance of the mass spectrometer probe has been improved, and significant advances in understanding the nature of its outputs have been made. Experimental determinations of chemical compositions in nonequilibrium airflows have been made that are at least as comprehensive as the thermodynamic measurements of Ref. 7 and appear to be equally successful. The increased capability of the instrument allowed systematic experimental determination of both NO and atomic oxygen concentrations and demonstration of the correlation of chemical composition with entropy. Divergence of the experimentally determined flow composition from that predicted for high reservoir entropy has been observed, primarily in the O_2/O system.

The electron beam technique is inherently limited to low pressure (< 1 torr) when quantitative analysis of the beam emission is required. The mass spectrometer must operate in even lower pressures (< 10^{-4} torr), but it appears that virtually any high-pressure source of usual aerodynamic interest may be successfully sampled and analyzed by appropriate changes in the sampling probe pumping system. (In a demonstration of high density operations, the existing mass sampling probe successfully admitted and analyzed static gaseous samples from sources with pressures as high as 2.6 atm.)

SECTION II
EXPERIMENTAL APPARATUS

2.1 18-IN. LOW-DENSITY WIND TUNNEL

The nonequilibrium air expansions that were subjected to mass spectrometric analysis in this investigation were produced in the arc-heated low-density wind tunnel described in Ref. 7 and shown in Fig. 1 (Appendix). A small stilling chamber was located downstream of a 250-kw d-c arc heater and served as a reservoir for a conical nozzle that exhausted into an open-jet test section. The test section was continuously pumped by a six-stage steam ejector. The dimensions of the expansion nozzle were: a throat diameter of 0.200 in., an exit diameter of 18 in., a conical half-angle of 10 deg, and a geometric exit-to-throat area ratio of 8100. Reservoir conditions produced for this test included stagnation pressures of 3.74 to 20.9 atm, stagnation temperatures of 2120 to 5380°K, and dimensionless entropy parameter in the reservoir (S/R) from 29.47 to 37.83. In the expanded flows at the nozzle exit, static pressure varied from 10 x 10^{-3} to 30 x 10^{-3} torr, and static temperature varied from 50 to 140°K.

2.2 GENERAL INSTRUMENTATION

The nozzle reservoir conditions were determined by the energy-balance technique, requiring precise measurements of heater input power, air mass flow, and power absorbed by the cooling water in all passages up to the throat. The heater input power was determined by voltage and current measurements at the heater electrodes. Power absorbed by the cooling water was determined by measuring volume flow rates of the water with a calibrated turbine-type flowmeter and measuring the temperature increases of the water with a ten-element thermopile. The air mass flow (0.01 to 0.05 lbm/sec) was determined

by measuring the pressure difference across a sharp-edged orifice with a strain-gage-type transducer. Inlet air temperature at the orifice was measured with a copper-constantan thermocouple.

The chemical composition was expected to be frozen well upstream of the nozzle exit and, hence, a function of the reservoir conditions only. There was, therefore, no reason to make extensive measurements of the usual type in the test section. The electron beam calibrations of Ref. 7 were assumed to be sufficiently accurate to provide the test section conditions (other than the flow composition).

2.3 QUADRUPOLE MASS SPECTROMETER

Only recently have mass spectrometers become commercially available in a size small enough for usefulness in probe studies of aerodynamic flows. The mass spectrometer selected for the research program described herein was one of the newer, compact types (a quadrupole) and is described completely in Ref. 15. Small physical size (4.5-cm-diam, 24-cm-long) and appropriate electrical features (high resolution, sweep times of a second or better, and single-mass monitoring) contributed to the selection of the particular instrument, a Quad 200® series manufactured by Electronic Associates, Inc., Palo Alto, California.

In operation, the quadrupole mass spectrometer performs the following functions: ionizes a small fraction of the incoming neutral sample particles, separates the ions by mass-to-charge ratio (m/e) through trajectory influence by a four-pole oscillating electrical field, and detects the ions surviving the separation process as a function of time. Over the three-year period of development of the sampling probe, the quadrupole was operated in essentially the original configuration except for the ion detector; i.e., the electron multiplier, discussed in Section 3.1.

2.4 FLOW SAMPLING PROBE

A comprehensive discussion of the flow sampling probe is presented in Ref. 15.

Physically, the probe was a cone-cylinder supported by a strut attached to a traversing arm with vertical and streamwise degrees of freedom. The dimensions of the probe were determined primarily by

the dimensions of the mass spectrometer; i. e., the probe merely served as a protective housing for the quadrupole head. The usual demands placed on a flow probe of surviving exposure to the flow and transmission of sensed information to a point external to the flow were satisfied without abnormal complexity. The probe was water cooled where required to ensure survival, and electrical operating and signal leads were protectively routed to ensure proper operation of the quadrupole.

There were two somewhat unique features of the probe: the sampling orifice and the liquid hydrogen cryopump. The sampling orifice diameter of 0.0254 cm was selected to be of the same order of magnitude as the mean free path of the flow and as sharp-edged as possible to ensure minimum disturbance of the flow sample. The orifice was located at the apex of the cone. The cone was of half-angle sufficient to decrease the orifice-to-ionizer distance, yet sharp enough to ensure an attached shock at the tip. Since minimum flow blockage was required, no diffusion pumps could be attached to the probe to pump the sampled flow and maintain the 10^{-4} torr environment required for proper operation of the quadrupole, hence a self-contained cryopump was designed for the probe. Liquid hydrogen was selected as the cryogen because of the need to pump all of the gases of interest in arc-heated airflow studies, and because of low-cost availability. An auxiliary mechanical pump was used to evacuate the interior of the probe to about 10^{-2} torr prior to filling the liquid hydrogen cryopump.

A section view of the probe is presented in Fig. 2.

2.5 AUXILIARY HIGH VACUUM CHAMBER

Both storage of the mass spectrometer head between runs and routine calibration of the instrument involved use of an available vacuum chamber that could be evacuated to 10^{-6} to 10^{-8} torr. The chamber was fabricated of 1-cm-thick mild steel in the shape of a cylinder 1 m in diameter and 3 m long. Several access ports were available for instrument mountings and feedthroughs. The chamber was evacuated first to a rough vacuum of 10^{-2} torr with a 23-liters (ℓ)/sec mechanical pump, then to 10^{-6} torr with a 1500-ℓ/sec oil diffusion pump. When necessary to attain a vacuum of 10^{-8} torr, further pumping action was provided by a liquid hydrogen cryopump of 10^5-ℓ/sec pumping speed.

For one of the access ports, a flange was used that allowed mounting side-by-side both the quadrupole segment of the sampling probe and an ionization gage for pressure measurement. Mounted in such a

manner, the ionization gage provided a close-proximity measurement of the pressure at the ionizer of mass spectrometer. A separate access port served as the point of injection for sample gases through a viscous leak valve.

Calibration of the mass spectrometer involved leaking into the chamber various single and multicomponent gas mixtures, followed by observation of the corresponding chamber pressure and spectrometer outputs. The gas mixtures were prepared and stored in a stainless steel container of about 1-ℓ volume that was connected to the input of the metering valve. A simple mercury manometer was used for the partial pressure measurements during preparation of the sample gas mixtures.

SECTION III
DEVELOPMENT OF AN OPERATING TECHNIQUE FOR THE MASS SPECTROMETER SYSTEM

Subsequent to the results reported in Ref. 15, a number of improvements were made in the mass spectrometer system. These improvements were of prime importance in the successful experimental determination of nonequilibrium composition.

3.1 THE RESISTANCE-STRIP MAGNETIC ELECTRON MULTIPLIER

From an operational standpoint, probably the single most important improvement was the change to a resistance-strip magnetic electron multiplier as an ion detector. The electrostatic venetian blind-type electron multiplier provided as the standard detector with the mass spectrometer was exceptionally sensitive to contamination. Exposure to the test gases of the arc-heated wind tunnel (at partial pressures exceeding 10^{-6} torr) produced order-of-magnitude decreases in output sensitivity, in some cases after only a few wind tunnel runs. A decontamination procedure was adopted but was time-consuming and, after several cleanings, ineffective.

A decision was made to replace the original detector with a resistance-strip magnetic electron multiplier that was reputed to possess high resistance to contamination. Both the original multiplier and the resistance-strip magnetic multiplier amplified the collected ion current by multiplication of secondary electrons ejected from the first dynode, or cathode, upon impact of the incoming ion, and both required

highly stable d-c voltages of from 1000 to 3000 v for proper operation. Beyond the cathode, however, internal differences in design accounted for great differences in operational usefulness. Within the original multiplier were fourteen separate dynodes, each fabricated of a copper-beryllium alloy. Exposure to corrosive gases, such as existed in the arc-heated air undergoing analysis, caused oxidation of the dynode surfaces, thereby substantially decreasing the yield of ejected secondary electrons, and hence decreasing the gain of the multiplier. The resistance-strip magnetic multiplier contained only two strips of glass coated with a high-resistance semiconductor material, instead of multiple dynodes. The secondary electrons ejected from the surface of the cathode upon impact of an ion were caused, by the influence of intersecting electrostatic and magnetic fields, to follow cycloid-like paths along the strip until collected by an appropriately placed anode. Upon each impact with the strip, additional secondary electrons were ejected, establishing large overall gain.

A more complete description of the resistance-strip magnetic multiplier is presented in Ref. 16.

Compared to the copper-beryllium dynodes, the strips were virtually immune to contamination. For fifteen months, the strip multiplier was operated without attention under severe environmental conditions, with only a 20- to 30-percent decrease in gain. During this time, 53 calibration runs and 46 runs in the arc-heated wind tunnel were made. Both the ionizer and the quadrupole rods required cleaning, but the strip magnetic multiplier was ignored. Such extended multiplier life was attributed to both the design features of the multiplier itself and an undemanding mode of operation. A preamplifier designed for use with the original multiplier was used with the strip magnetic multiplier also. With increased amplification at high signal-to-noise ratio, it was possible to limit the voltages applied to the strips to 800 to 1200 v, or about 40 to 60 percent of the maximum suggested by the manufacturer. Consequently, the anode current was limited to approximately 0.1 μa, or about 50 percent of the suggested maximum.

3.2 DETERMINATION OF COMPOSITION FROM MASS SPECTRA

In the ionizer section of the mass spectrometer, incoming sample particles are bombarded by a beam of electrons, and a small fraction is ionized. Ionization of the neutral sample particles is necessary for mass discrimination by the rf d-c field of the quadrupole section to be effective and unfortunately complicates analysis of the output currents

when polyatomic molecules are involved. Under certain operating conditions in the ionizer, viz. when the energy of the bombarding electrons is high enough to produce large numbers of ions and hence a large signal-to-noise output, a polyatomic molecule may undergo single ionization, multiple ionization, or dissociation with ionization of the constituent atoms or radicals (dissociative ionization). For example, impacts of electrons of 90-v energy with nitrogen molecules (N_2) produce not only the predominant singly ionized molecule, N_2^+ (m/e = 28), but also the singly ionized atom, N^+ (m/e = 14), and the doubly ionized molecule, N_2^{++} (also m/e = 14). Such encounters produce an output current at m/e = 14 that is some 8 to 10 percent of the output current at m/e = 28, the "parent" peak. If only the abundance of N_2 in a sample is desired, then the fraction lost to dissociation and multiple ionization is negligible. However, if the output current at m/e = 14 is to be examined for evidence of the existence of atomic nitrogen in the sample, then the total output current at m/e = 14 must be corrected for the contribution of N^+ and N_2^{++} ions originating in dissociative ionization and double ionization of the N_2 molecules in the sample.

A general expression for total output at m/e = i is:

$$I_i = \sum_{j=i}^{n} c_{i,j}\, n_j \tag{1}$$

where I_i is the output signal at m/e = i, n_j is the number density of particles of mass j, and $c_{i,j}$ is the absolute sensitivity of the mass spectrometer to ions produced at m/e = i from parent particles of mass j. The summation begins at i because a parent particle cannot yield a fragment ion of greater m/e than itself. The summation extends over the entire range of mass numbers known or suspected to be in the sample. By assuming that the sensitivities ($c_{i,j}$) are known by calibration or otherwise (many will be exactly zero), the sample composition is obtained from the measured I_i in the mass spectrum by simultaneous solution of the system of linear algebraic equations, Eq. (1). In the general case, a machine solution is required, but manual solutions are possible in many cases in which the sample contains relatively few components and many of the $c_{i,j}$ are zero. For the case discussed herein, i.e., a low-density air plasma expanded from no more than 5000°K, finite rate calculations indicate that only N_2, O_2, NO, N, and O need be considered as significant constituents. The outputs corresponding to the m/e of the singly ionized molecular species are all single-component so that the abundances of these species are obtained simply from the total I_i and appropriate $c_{i,j}$:

$$n_{O_2} = I_{32}/c_{32,32}$$

$$n_{NO} = I_{30}/c_{30,30} \qquad (2)$$

$$n_{N_2} = I_{28}/c_{28,28}$$

To obtain the densities of atomic species, the appropriate output signals must be corrected for the (spurious) contributions of ionized products of dissociation of heavier particles:

$$n_O = \frac{I_{16} - I_{16,32} - I_{16,30} - I_{16,18}}{c_{16,16}}$$

$$(3)$$

$$n_N = \frac{I_{14} - I_{14,30} - I_{14,28}}{c_{14,14}}$$

The corrections to the I_{16} output account for the contributions of dissociative ionization of O_2, NO, and H_2O, respectively, where H_2O is necessarily included as a known contaminant in the wind tunnel flow. The corrections to the I_{14} signal represent contributions of dissociative ionization of NO and N_2, respectively.

Care must be taken to limit the outputs of interest to the major species in a given sample to prevent the data reduction from becoming unnecessarily complex. Most mass spectrometers are so sensitive that not only are the major constituents readily detected, but also many other species of negligible contribution. The mass spectra of low temperature air at high and low sensitivity are compared in Fig. 3. The relative simplicity of the low gain spectrum is easily seen when compared with the complexity of the high gain spectrum where various isotopic and doubly ionized species become detectable. In the wind tunnel test, outputs of m/e = 40, 44, and 46, corresponding to A, N_2O, and NO_2 were neglected as trace components.

3.3 OUTPUT REPEATABILITY, EFFECT OF CONTAMINATION

A major obstacle to the analysis of mass spectra as outlined in the previous section was the fact that the absolute or total sensitivity coefficients ($c_{i,j}$) measured in static calibrations were not sufficiently repeatable to give quantitative results in the usual sense. In Fig. 4, the absolute sensitivity of the m/e = 28 output ($c_{28,28}$) in an air sample (in this case based on partial pressure rather than number density) is presented as it varied with serial run number during a calibration sequence in which the system was known to be clean and uncontaminated. Variations

of up to 100 percent between successive calibration points can be seen. Such variations could be accepted for wind tunnel testing by calibrating prior to each tunnel run. However, the variations of up to 50 percent during some individual runs could not be similarly accepted, apparently limiting the absolute approach to accuracies of no better than 50 percent. Thus, even in a clean system, quantitative use of the mass spectrometer with absolute or total calibration factors for pure gases is not feasible with the present equipment.

In a contaminated system, the absolute sensitivity was even more unreliable. A progressive deterioration was observed although a "contamination threshold" was often observed with extremely sharp decreases in reliability. In Fig. 5, the absolute sensitivity parameter ($c_{28,28}$) is presented as a function of electron energy for both a clean system and a grossly contaminated system. The points at 90 v correspond to the points of Fig. 4 for Run No. 80. The ionizer section of the spectrometer had been cleaned immediately prior to this run. From Fig. 5, it can be seen that in Run No. 79, the last run before cleaning, extensive hysteresis in the variation of the absolute sensitivity parameter occurred, creating uncertainties of well over two orders of magnitude.

Fortunately, the observed behavior of relative outputs under contaminated conditions was much better. Consequently, the entire mass analysis procedure was put on a relative basis, as described in Section 3.5. Even then, a certain amount of discretion was necessary. Two categories of behavior were observed, one for simple undissociated ions and one for dissociated ions. The lower curves in Fig. 5 demonstrate that the relative output sensitivity of simple undissociated ions displayed good repeatability (±1 percent) in a clean system, and acceptable repeatability (±4 percent) in a grossly contaminated system (note that the two curves are plotted on a linear rather than a logarithmic scale). For a state of spectrometer contamination that causes a decrease in absolute sensitivity by a factor of 100, the ±4-percent repeatability of the relative outputs of O_2 and N_2 in air was remarkable. No hysteresis loops were formed.

When analyzing samples containing dissociated ions, the repeatability of the relative sensitivities of dissociated ions became important. These relative sensitivities were observed to be strongly affected by contamination, although not as drastically as was the absolute sensitivity. The middle curves of Fig. 5 reveal that the relative sensitivity of N^+_{14} to N^+_{28} in air was repeatable to about ±4 percent in a clean system, but in the contaminated system, hystereses of as much as an order of magnitude occurred. When such a sample was to be analyzed, the system

had to be reasonably clean, and further, the state of contamination required continuous monitoring by observation of the I_{14}/I_{28} ratio in an air sample. In Fig. 6, it is seen that the contamination effect began at the lower electron energies and progressed to higher electron energies. In practice, all wind tunnel test data were obtained at V_{ee} = 90 v, which maximized the time between required cleaning of the ionizer.

In summary, the calibration studies indicated that relative measurement of nondissociated species could be made with expected repeatabilities of from 1 to 4 percent, depending on the amount of attention given to ionizer cleanliness. Relative measurements involving dissociated ions could be made to at best only 4-percent repeatability, and to achieve even this level of repeatability required frequent assessment of the state of ionizer cleanliness by means of calibrations between runs.

3.4 NATURE OF CONTAMINATION AND THE DECONTAMINATION PROCESS

The "contamination" that has been identified as the cause of the poor repeatability of certain output parameters has not been described or defined. The detailed nature of this contamination is not known with certainty, but it is thought to be attributable to adsorbed molecules on the interior surfaces of the mass spectrometer, primarily in the ionizer. In an advanced state of contamination, such deposits are visible to the eye as very thin, light brown layers of unknown composition. It is believed that these deposits are primarily fractionated components of diffusion pump oil, although the state of contamination is known to be greatly aggravated by certain test gas molecules; e. g., nitric oxide. Nor is the exact effect of the deposits on the mass spectrometer operation known. It is theorized that the contamination deposits act as an insulator which can accumulate electrical charge at random locations inside the ionizer. Since the ionizer is designed for field-free diffusion of ions from the point of formation in the electron beam to the exit aperture of the ionizer, it is plausible that random potential fields inside the ionizer, produced by random charge accumulation, could so perturb the ion trajectories that unrepeatable mass discrimination within the ionizer would result. It is also plausible that in extreme cases the ion trajectories could be so badly distorted that there would be order-of-magnitude decreases in ion supply to the mass analyzer.

Whether or not the above is an accurate description of the contamination mechanism, it is a practical fact that the cleaning procedure which was designed to restore the interior metallic surfaces of the mass spectrometer to clean metal was completely effective in elimination of the

"contamination effect." All components of the spectrometer requiring decontamination were either stainless steel or ceramic. Since the ceramic insulators were fragile and porous, no attempt was made to clean them; they were replaced as necessary. Removal of the contaminating deposits from the stainless steel components was accomplished with a fine grain pencil eraser (Pink Pearl® or equivalent), followed by a 30 min to one hour rinse in a solution of Freon TF® vibrating at ultrasonic frequency. (An intermediate step of soaking the scrubbed parts in phosphoric acid prior to the rinse was added late in the research program. Considerable improvement in cleaning efficiency resulted.) Assembly of the cleaned components was accomplished with the use of plastic gloves, thereby avoiding recontamination through human contact.

3.5 RELATIVE BINARY CALIBRATIONS

The relative approach to analysis of mass spectra requires knowledge of the ratios of the absolute sensitivity factor ($c_{i,j}$). In most cases, these ratios are easier to determine and are much more reliable than the absolute values of the individual sensitivity factors. There are at least three types of these relative sensitivities which are of concern, identified as relative binary calibration factors.

3.5.1 $c_{i,i}/c_{k,k}$, Both Species Are Undissociated Ions

When the desired concentration ratio involves only simple undissociated parent ions, the individual concentrations are given by expressions of the form of Eq. (2), and the relative concentrations are clearly given by the ratio of relative outputs at the appropriate m/e, I_i/I_k, divided by the relative calibration factors $c_{i,i}/c_{k,k}$. Generally, the concentration of N_2 is used for normalizing so that the relative calibration factors have the form $c_{i,i}/c_{28,28}$. These factors were obtained by direct experimental measurement of relative sensitivities in known sample mixtures. An accurately known mixture available in unlimited quantity was air itself, from which the ratios $c_{32,32}/c_{28,28}$ and $c_{40,40}/c_{28,28}$ were easily obtained. Relative calibrations involving NO were obtained by preparing a mixture of approximately 50 percent NO and 50 percent A and introducing it in a controlled manner into the auxiliary high vacuum chamber. The resulting $c_{30,30}/c_{40,40}$ was converted to $c_{30,30}/c_{28,28}$ by simple multiplication. The NO/N_2 calibration was not obtained directly because of possible reactions in the required sample mixture.

3.5.2 $c_{i,j}/c_{j,j}$, One Species a Dissociated Fragment of the Other

Relative calibration factors of this type are required to correct output signals for the contributions of dissociative ionization. For example:

$$\frac{n_N}{n_{N_2}} = \left(\frac{I_{14}}{I_{28}} - \frac{I_{14,30}}{I_{30,30}} \times \frac{I_{30}}{I_{28}} - \frac{I_{14,28}}{I_{28,28}}\right) \div \left(\frac{c_{14,14}}{c_{28,28}}\right) \tag{4}$$

where

$$\frac{I_{14,30}}{I_{30,30}} = \frac{c_{14,30}}{c_{30,30}}$$

and

$$\frac{I_{14,28}}{I_{28,28}} = \frac{c_{14,28}}{c_{28,28}}$$

since the same parent species produces the ion output current in the numerator and denominator in each case. This also means relative calibration factors of this type can be obtained in unknown mixtures, requiring only the presence of a sufficient partial pressure of the parent species. This type of relative calibration factor is commonly known as the fragmentation factor. For a given parent species, a family of fragmentation factors is called the cracking pattern for that species. These factors, as the previous ones, are obtained experimentally with a high degree of accuracy.

3.5.3 $c_{i,i}/c_{k,k}$, One Species in a Dissociated Fragment of the Other

This type of relative calibration factor, represented by the factor inside the second brackets of Eq. (4), is the most difficult to obtain, since, in most cases, the dissociated fragment is not stable at room temperatures. It is virtually impossible to prepare a known mixture containing such components. An example is the $c_{14,14}/c_{28,28}$ factor in Eq. (4), since atomic nitrogen (m/e = 14) is not stable at room temperature. Because of this, the two relative calibration factors of this type that were required in the wind tunnel mass analysis ($c_{14,14}/c_{28,28}$ and $c_{16,16}/c_{32,32}$) were not measured experimentally but were obtained by reference to values of ionization cross section of atomic oxygen and nitrogen reported in scientific literature. The relation between ionization cross section and the absolute sensitivity factors is expressed by:

$$I_{i,j} = (n_j i_e L_{eff} \sigma_{i,j}) \times F_i = n_j c_{i,j} \tag{5}$$

from which it follows that the $c_{i,j}$ are directly proportional to the ionization cross section:

$$c_{i,j} = i_e L_{eff} \sigma_{i,j} F_i \tag{6}$$

and that

$$\frac{c_{i,i}}{c_{k,k}} = \frac{\sigma_{i,i}}{\sigma_{k,k}} \frac{F_i}{F_k} \tag{7}$$

The relative ionization cross sections for O and N, relative to O_2 and N_2, respectively, are given in Ref. 17:

$$\frac{\sigma_{16,16}}{\sigma_{32,32}} = 0.781 \text{ and } \frac{\sigma_{14,14}}{\sigma_{28,28}} = 0.654 \text{ at } V_{ee} = 90 \text{ v} \tag{8}$$

The nature of the variation of the instrument factor (F_i) with species is not clear. This factor is essentially a function of the type of electron multiplier response. Two limiting cases are frequently described, viz., a strict ion energy dependence, that results in an F_i independent of mass, and an ion velocity dependence, that results in an F_i varying as $(M_i)^{-1/2}$. The wind tunnel data supported the mass-independent case, based on an overall atom balance for oxygen atoms.

Because of the additional uncertainties involved in the relative calibration factors required for determination of atomic oxygen and atomic nitrogen concentrations, it is clear that these components will not be determined with as much accuracy as are the molecular components.

3.6 APPLICATION OF BINARY CALIBRATION FACTORS IN A COMPLEX STATIC SAMPLE

The applicability of the binary calibration factors to more complex samples was evaluated by submitting a four-component static sample of O_2, N_2, A, and CO_2 to mass analysis. An oscilloscope picture of the spectrum is shown in Fig. 7 for two different signal amplifications. Only the outputs at m/e = 28, 32, 40, and 44 were required to analyze the sample; however, dissociative ionization corrections were required at m/e = 28 and 32 because of dissociation of CO_2 in the ionizer. A comparison of the sample composition as prepared and the composition determined by the mass spectrometer is given in Fig. 8 and in the following table:

Component	Prepared Sample	Mass Spectrometer	Difference, percent
N_2	0.5489	0.5447	-0.42
CO_2	0.2402	0.2392	-0.10
A	0.0990	0.1060	+0.70
O_2	0.1119	0.1099	-0.20

SECTION IV
WIND TUNNEL TEST PROCEDURE

The results of Ref. 18, showing that nonequilibrium effects correlate with reservoir entropy, influenced the test program run schedule. That is, with an S/R correlation expected as a final result, no effort was made to achieve specific stagnation temperatures, and nominal stagnation pressures of 5, 10, 15, and 20 atm were set merely as a convenience. In this manner, a range of values of the dimensionless reservoir entropy of 29.5 to 37.8 was covered. The reservoir state at each operating point was established by measuring p_{t_1} and calculating the stagnation enthalpy using the energy balance technique. In Ref. 7, it was shown that such calculations agreed with sonic flow enthalpy within ±8 percent.

The sequence of operation for each mass spectrometer run began with evacuation of the test section and nozzle to approximately 1.5×10^{-2} torr utilizing the steam ejector. During this operation, the mass sampling probe was positioned outside the flow boundary with the inlet orifice capped and with an internal vacuum of from 10^{-3} to 10^{-2} torr established by an auxiliary mechanical pump. Prior to firing the arc heater, liquid hydrogen flow was established to the cryopump within the probe. After firing the heater and establishing "stabilized" conditions in the arc heater, generally in less than a minute, the probe cap was removed using an hydraulic actuator. The probe was then traversed into the flow, stopped at a desired point, and a number of mass spectra recorded. The time period of immersion in the flow varied from 3 to 8 min. When stagnation conditions were such that probe heating was critical, the heater flow was terminated before probe retraction, thereby minimizing exposure to the flow.

Although the long-term stability of the arc-heater operation was good, high frequency fluctuations in voltage and current remained after the starting transient, as is typical of high-pressure arc heaters. These fluctuations were probably responsible for some high-frequency disturbances observed simultaneously in the mass spectrometer outputs, particularly at the m/e ratios corresponding to the high temperature components, NO and O. Similar fluctuations have also been observed in other types of diagnostic measurements in the same flows and have necessitated a time-average approach to the data reduction process. The mass spectrum was monitored continuously during a run by an oscilloscope (1 sweep/sec), and test data were recorded when desired on an oscillograph (1 spectrum/sec). A sufficient number of spectra

were recorded at each test point to provide data for a valid time-average. Over the period of a typical oscillograph record (6 to 8 sec), ±20-percent fluctuations in O and NO were observed, while the N_2 and O_2 signals changed by only ±7 percent.

The run time was determined by the probe heating rate at the most forward O-ring location on the probe. A temperature of 400°F was set as a limit for most runs to protect the O-rings used to seal access joints in the probe. After obtaining most of the data reported herein, several long runs were made to obtain boundary layer specie profiles. During these runs, the temperatures at the most forward O-ring increased to as high as 505°F without detectable damage to the probe or the O-rings.

SECTION V
TEST RESULTS

5.1 TYPICAL SPECTRA

By using the mass spectrometer probe, the frozen compositions in the expanded flow of the 18-in. wind tunnel were determined for a range of stagnation pressures of from 3.7 to 20.8 atm and stagnation temperatures of from 2120 to 5380°K.

The finite rate expansion calculations predict, for increasing temperature, an O_2 concentration decreasing with respect to N_2, increasing O and N concentration, and a peaking behavior of NO. Two sample mass spectra are given in Fig. 9, one for a low reservoir temperature, and one for a high reservoir temperature. The decrease in O_2 and increase of NO and O relative to N_2 is evident at the higher temperature. The appreciable output signal at m/e = 14 is almost entirely the contribution of dissociative ionization of N_2 in the ionizer. When this contribution is subtracted from the total m/e = 14 output signal using calibration data, very little signal remains to attribute to atomic nitrogen in the sample. This is in qualitative agreement with the finite rate calculation prediction of less than 0.003 mole fraction of N for the above range of reservoir conditions. On the other hand, the output signal at m/e = 16 (for T_{t_1} = 5000°K) represents almost entirely atomic oxygen. From calibration data, it was known that only about 10 percent of the already small signal at m/e = 32 would contribute to the signal at m/e = 16 through dissociative ionization.

5.2 ENTROPY CORRELATION

It was demonstrated in Ref. 18 that the nonequilibrium compositions in high enthalpy nozzle expansions calculated by finite rate theory may be correlated with the reservoir entropy. It was determined that the experimental composition measurements described herein did also. All of the mass spectra data for the molecular species N_2, O_2, and NO, reduced to mole fraction form, are presented in Fig. 10a. The same type of entropy correlation is given for the atomic species, O and N, in Fig. 10b.

The broken-line curves are the results of the finite rate calculations of Marshall (Ref. 7) and are in very close agreement with the correlation curves of Ref. 18, except for NO at $S/R < 33$. In the flow model of Ref. 7, air was considered a mixture of five species, N_2, O_2, NO, O, and N. The energetically important dissociation/recombination reactions for N_2, O_2, and NO, as well as the NO shuffle reactions, were included in a system of 18 coupled finite-rate chemical reaction equations. In addition, finite rate vibrational energy exchanges were included for the three diatomic molecules. The thermodynamic predictions of this theory were satisfactorily verified by the electron beam measurements in Ref. 7. The solid-line segments of the theoretical curves represent from left to right the finite rate solutions for various ranges of stagnation pressure at constant stagnation temperatures of 2300, 3000, 4000, and 5000°K. The dashed lines are simply fairings of the theoretical values between the constant temperature segments.

The experimental points are identified with respect to the nominal value of stagnation pressure set for that point (5, 10, 15, 20 atm). Each data point represents a time average over at least six mass spectra (~ 6 sec) during a single run at stabilized arc-heater conditions. All points were obtained in the inviscid test core at distances of 2 to 3 in. from the nozzle centerline. The test data were corrected for the effects of dissociative ionization at $m/e = 14$ and 16, as well as a mass separation or migration within the sampling probe.

5.3 BOUNDARY LAYER MEASUREMENTS

It was originally intended to obtain composition profiles through the nozzle boundary layer by means of continuous traverses with the mass spectrometer probe. The unforeseen need to perform time-averages of the data, however, as indicated in Section IV, made such a procedure impossible. Instead, during a given run, the probe was moved step-by-step through the boundary layer in increments of one inch. At each

incremental point, from six to twelve mass spectra were recorded to provide a basis for a time-average. This procedure not only increased the required run time, but also greatly increased the effort required in data reduction. Therefore, only a limited amount of such data was obtained. A sample distribution of the specie concentrations across the upper half of the exit plane of the nozzle for p_{t_1} = 5.03 atm and T_{t_1} = 4870°K is presented in Fig. 11. The composition was constant in the inviscid core but varied considerably, though systematically, throughout the boundary layer.

SECTION VI
DISCUSSION

6.1 GENERAL

The foremost impression gained upon examination of the experimental determination of specie concentrations is that a systematic correlation with the entropy parameter indeed exists, just as with the results of the theoretical calculations. In this respect, the cluster of test points at S/R = 30.5 is notable, since the compositions are essentially repeated for a wide range of reservoir pressure and temperature. This correlation of frozen compositions is of considerable value in analyzing and organizing the chemical nonequilibrium effects in wind tunnel nozzle flows.

A second major impression is that the general trends predicted by theory are confirmed experimentally, in particular the peaking behavior of the nitric oxide mole fraction. The theoretical values are not reproduced perfectly, however. Specifically, it is noted that the concentrations of the three molecular species (N_2, O_2, and NO), together constituting over 85 percent of the total flow sample, are in good agreement with the finite rate predictions at low values of entropy; i.e., flows of small nonequilibrium effects. But, at S/R ≅ 32, a divergence begins, with the O_2 fraction increasing with respect to the theory by some 6 to 7 percent of the total sample and the NO fraction of the total sample reaching a value about 3 percent greater than predicted. Note that, because of the logarithmic nature of the mole fraction scale, the N_2 fraction appears to agree very closely with the finite rate theory; but in reality, the N_2 fraction is also greater than the predicted value by about 2 to 3 percent of the total sample. Aside from these minor differences, the molecular data are very consistent over the entire entropy range covered and tend to display the same general shapes as do the theoretical curves.

In addition, the two atomic fractions, N and O, are not in as good agreement with the theoretical prediction. Calculations indicate that the atomic nitrogen fraction is negligible (below the 0.003 detectability limit) for the selected range of reservoir entropy. The experimental program generally confirmed this, although atomic nitrogen was apparently detected in a few separate runs at high stagnation temperature (Fig. 10b). It is not certain whether these were valid detections, or simply the result of inaccuracies in applying the dissociative ionization correction to the output signal at $m/e = 14$.

The atomic oxygen fractions, however, were readily observed and ranged from the detectability limit at low entropies to approximately 0.23 mole fraction at the highest entropy. The atomic oxygen measurements were very self-consistent over the entire entropy range but were systematically lower than the theoretical predictions. Although the discrepancy was only 1/2 to 9 percent with respect to the total sample, it amounted to 30 to 50 percent of the predicted O fraction. Also, the scatter of the atomic oxygen data is noticeably greater than for the molecular data. This agrees with the results of the repeatability studies performed during the static calibration tests (Section 3.3).

6.2 POSSIBLE EXPLANATIONS OF DISCREPANCIES BETWEEN EXPERIMENT AND FINITE RATE EXPANSION THEORY

Several possible explanations exist of the discrepancies between the mass spectrometer measurements and the finite rate theory (primarily the O_2 and O measurements at high entropy). Three general categories of explanations are discussed here in order of what is judged to be increasing probability.

6.2.1 Mass Separation in the Nozzle Expansion

It is well known that low-density, free-jet expansions exhibit mass separation (Ref. 19). Low-density nozzle flows may also. The discrepancy noted above in the O/O_2 measurements is in the direction characteristic of mass separation; that is, an indication of reduced concentration of light particles (0), with a corresponding indication of increased concentration of heavy particles (N_2, O_2, NO), near the axis of the flow. Also, the largest indication of increased concentration occurs for the heaviest particle of interest, O_2. However, the limited amount of data obtained during traverses of the exit plane of the nozzle (inviscid core plus boundary layer)(Fig. 11) reveals variations in composition inappropriate for an explanation of mass separation in the nozzle flow. In fact, composition in the inviscid core was determined to be very

nearly constant (Fig. 11), while concentration of the lighter component (O) in the boundary layer was found to decrease with distance from center of the flow, presumably because of increased collision-induced recombination in the boundary layer.

6.2.2 Errors in the Mass Spectrometer Probe Measurements

As a new instrument, the mass spectrometer probe is certainly due close examination on several points. Among these are possible mass separation within the probe, accuracy of the probe calibration factors, and validity of the application of room temperature calibrations to samples having elevated vibrational temperatures.

Mass separation inside the probe was considered in the data reduction process by assuming that free molecule diffusion conditions apply in the stream tube admitted to the probe. Since, for the i^{th} species, the diffusive velocities away from the stream tube centerline ($\bar{v}_i$) are proportional to $1/\sqrt{M_i}$, then the flux per unit area of the i^{th} species at the ionizer inlet aperture was different from that at the probe inlet by a factor proportional to M_i. An appropriate correction was applied to the test data to compensate for this effect.

The relative probe calibrations for molecular species were as accurate as could be made within the demonstrated experimental calibration repeatability limits of a few percent. The relative calibration factors involving the atomic species, on the other hand, were less well established. As discussed in Section 3.5, the relative atomic calibration factors were not obtained experimentally but were based on values of the ionization cross sections of O and N relative to O_2 and N_2 as reported in the scientific literature. Intuition and theory both suggested that the atomic cross sections should be on the order of one-half the cross sections of the parent molecules, and the reported values clearly fell in this range; e.g., $\sigma_{16,16}/\sigma_{32/32} = 0.781$ (see Section 3.5). However, since the values were based on a limited number of experiments, the accuracy was questionable. In fact, the atomic oxygen discrepancy at high entropy could be essentially eliminated by arbitrarily reducing $\sigma_{16,16}/\sigma_{32,32}$ to exactly 0.50, but to eliminate the discrepancy in the middle range of entropy required a reduction to 0.31, which was tantamount to assuming the reported values to be in error by 60 percent. Furthermore, this arbitrary alteration in ionization cross section for O relative to O_2 would have no effect on the O_2 mole fractions, whereas the measured discrepancies in O_2 and O strongly suggested a related and apparently opposite effect on these fractions.

There is also a question concerning the applicability of the room-temperature probe calibrations to samples obtained at elevated vibrational temperatures. Vibrational temperatures of 1800 to 2900°K have been measured in the nozzle test flows (Ref. 7) and would be expected to persist in the flow sample admitted to the probe. The probable effect of such high vibrational temperatures in the sample would be to facilitate dissociation, but not ionization, hence the molecular measurements that depend on simple ionization in the ionizer would not be affected. Dissociative ionization, however, could conceivably be enhanced, resulting in an increase in the indicated atomic mass fractions. Since the atomic oxygen discrepancy has been detected in the opposite direction, it appears reasonable to eliminate vibrational temperature effects from consideration.

6.2.3 Inaccuracy of the Finite Rate Calculations

Even though the thermodynamic measurements of Ref. 7 appear to substantiate the finite rate calculations, there are still several points upon which the finite rate model may be questioned. In the first place, the relative concentrations of O and O_2 determined with the mass spectrometer probe appear to have been verified by several independent experiments using entirely different measuring techniques. Recent catalytic probe measurements, although displaying significant scatter, indicated that the atomic oxygen concentration in shock tunnel expansions of air was much lower than the predictions of finite rate calculations (Ref. 11). A similar result has been obtained from observations of the oxygen components of radiation from an electron beam in a nonequilibrium airflow.

In the second place, there are certain parts of the finite rate calculations that can be questioned directly. From a phenomenological standpoint, even though the present calculations do appear to account for all of the important physical processes occurring in rapid finite-rate expansions (with the possible exception of coupling of vibration and dissociation, an effect that would produce trends opposite to the observed discrepancies), the state of knowledge of the required high temperature reaction rates is far from satisfactory. The rates used herein were cited by Gavril (Ref. 20) from an original summary by Steiger (Ref. 21).

In Fig. 10, the indication that the discrepancies between the experimentally determined O/O_2 concentrations and theory are much greater than for the other species in the flow is highly suggestive of a prior observation that the chemical kinetic system of oxygen is effectively isolated. Such a conclusion was made in Ref. 22; i.e., that the nitrogen and nitric oxide concentrations in finite rate air expansions were determined almost entirely by the fast (two-body) nitric oxide shuffle reactions,

while the oxygen concentrations were determined solely by the slower (three-body) oxygen dissociation-recombination reactions. Together with this conclusion, the present experimental results suggest, then, that the rates used in the calculations for the two bimolecular shuffle reactions (Nos. 16 and 17 of Table II in Ref. 7) are much more accurate than those used for the oxygen dissociation-recombination reactions (Nos. 1 through 5, Table II of Ref. 7). Indeed, a recent summary of reaction rate data (Ref. 23) indicates that the original experimental data that furnished the rates of the shuffle reactions are much more consistent over an extensive range of temperature than are any of the corresponding data for the termolecular reactions.

An attempt was made to determine what changes in the oxygen reaction rates would be required to bring the calculated results into agreement with the experimental results. Two new finite rate calculations were performed with the reaction rates of the five oxygen dissociation-recombination reactions

$$O_2 + M \underset{k_b}{\overset{k_f}{\rightleftarrows}} 2O + M, \quad M = N_2, O_2, NO, N, O \tag{9}$$

increased by factors of 10 and 100, respectively, over the rates of Ref. 7. These calculations were made for only two reservoir conditions: p_{t_1} = 10 atm, T_{t_1} = 4000°K, S/R = 33.6 and p_{t_1} = 5 atm, T_{t_1} = 5000°K, and S/R = 37.0. The results are presented in Fig. 12, superimposed on the bands of experimental data from Fig. 10. Curves have been faired through the new calculations so as to be approximately parallel to the curves for the original reaction rates. It can be seen that multiplying the original rates by 100 virtually eliminated the experimental/theoretical discrepancy. The rate increases affected primarily the oxygen concentrations, but there were also small increases in the nitric oxide fractions, indicating that the oxygen system is not entirely chemically independent.

As a result of these calculations, the question naturally arises as to whether the original experimental measurements of the oxygen dissociation rates could have been made in error by two orders of magnitude. If it is assumed that the measurements were basically valid and subject only to the usual experimental scatter, then such a sizable error is not likely. The experimental rate data taken in different laboratories (Ref. 23) agree within a maximum scatter band of 400 percent, and in most cases within 200 percent. The possibility that a considerable number of independent investigators made experimental errors of up to several thousand percent in the same direction must be considered as quite remote.

On the other hand, if the viewpoint is taken that the reaction rate experiments are all subject to fundamental uncertainties of interpretation in addition to the usual experimental scatter, as is readily admitted by many investigators in the fields, then it appears that errors of 100x are quite possible. The kinetics of a simple dissociation-recombination reaction, such as Eq. (9), are usually represented by the following expressions

$$k_f = c_f T^{\eta_f} e^{-\theta_D/T} \tag{10}$$

$$K_c = k_f/k_b \tag{11}$$

In the present case, Eq. (11) may be seriously questioned as an adequate description of the relationship between the forward and reverse reaction rates. The question is pertinent because of the manner in which the two reaction rates affect the finite rate calculations. In finite rate nozzle expansions, the dissociation rates rapidly decrease to a negligible fraction of the recombination rates (because of exponential dependence on temperature), hence the high temperature recombination rates essentially determine the composition of the flow. Unfortunately, however, there are no experimental sources for such rates. To date, recombination rates have been measured only in low temperature experiments.[1] The required high-temperature recombination rates for nozzle calculations are inferred from high temperature dissociation rate measurements, using the equilibrium constant and Eq. (11). This procedure is questionable because, with very few exceptions, such derived high temperature recombination rate data, when extrapolated to low temperatures, disagree by orders of magnitude with low temperature recombination rate measurements (see Ref. 23). (It is interesting to note that the uncertainty over the use in nozzle flow calculations of high temperature recombination rates derived from measured dissociation rates has a direct parallel in the behavior of vibrational relaxation in similar expansions. It was discovered a number of years ago (cf. Refs. 7 through 10) that vibrational rates measured in shock wave experiments do not apply in rapid nozzle expansions where the approach to equilibrium is from the opposite direction.)

---

[1]A single possible exception is the experiment of Ref. 24, in which oxygen recombination rates were measured directly at 3000°K by observing O_2 absorption downstream of a sudden expansion in a shock tube. It is noted that these measurements were made near equilibrium but were analyzed with a reaction equation in which the dissociation rate was zero—a procedure that would underestimate the recombination rates.

There is the additional question of the propriety of applying Eq. (10) to nonequilibrium flows since the derivation is based on equilibrium collision rate theory. In fact, in Ref. 23, Bortner has noted that some attempts to fit empirical data for oxygen to Eq. (10) force severe contradictions of the collision rates derived from equilibrium kinetic theory.

In summary, it is considered that, of the possible explanations for the discrepancies noted in Fig. 10, the most cogent is the lack of well-substantiated termolecular recombination rates for oxygen in the high temperature regime of importance in determining the O/O_2 concentrations in finite rate expansions. There may also be inaccuracies in the corresponding termolecular rates for N_2 and NO, but not serious enough to affect the final N_2, N, and NO concentrations. The concentrations of these species are determined by the nitric oxide shuffle reactions. The experimental data reported herein indicate that the rates used for the shuffle reactions are accurate.

SECTION VII
CONCLUSIONS

The results of an on-line mass spectrometric analysis of nonequilibrium airflows may be summarized as follows:

1. A mass spectrometer sampling probe has been developed to make possible reliable determinations of the chemical composition in nonequilibrium flowing gases.
2. Frozen compositions in a low-density expansion of air in an arc-heated wind tunnel were determined for reservoir pressures of from 3.7 to 20.8 atm and reservoir temperatures of from 2120 to 5380°K. The empirically determined compositions were correlated with the reservoir entropy. At low entropy, the molecular concentrations were in agreement with predictions of finite rate theory. At high entropy, molecular concentrations were greater than predicted, by as much as 7 percent for O_2. The atomic oxygen concentration was observed to be consistently less than the predicted values over the entire entropy range, and at the highest entropy was 9 percent less than the expected value.

3. Finite rate calculations were made with increased oxygen reaction rates. Increases of 100 times were required to bring the predicted concentration of O_2 and O into agreement with the experimentally determined values.

4. It is considered that the most probable explanation of the discrepancy between predicted and experimental oxygen concentrations is the reliance in the calculations upon high temperature three-body recombination rates for oxygen which are not substantiated by direct experiments but which are derived from high temperature dissociation rates. The much better agreement with theory of the nitrogen and nitric oxide concentrations is considered to be evidence of a high degree of accuracy of the reaction rates used for the nitric oxide shuffle reactions as well as a virtual chemical kinetic isolation of oxygen.

5. Flow composition was determined in the nozzle boundary layer for a limited number of cases. A uniformity of composition in the inviscid core was demonstrated, but considerable variation in the species concentrations in the boundary layer was detected.

6. No better than 50-percent repeatability could be demonstrated when the mass spectrometer probe was used to determine absolute concentrations. Determination of relative concentrations was then adopted for use in the wind tunnel, since repeatability of relative output sensitivity was demonstrably better. For example, for simple nondissociated species, the repeatability in a clean system was determined to be 1 to 4 percent, while for dissociated species, the relative sensitivity was not quite as repeatable (4 to 10 percent), but still adequate for quantitative work.

7. Cleanliness of the mass spectrometer system was the fundamental determinant of repeatability. Continued exposure to chemically active hot gases necessitated periodic cleaning of the ionizer section of the spectrometer. A resistance-strip magnetic electron multiplier was adopted for use with the mass spectrometer and proved to be virtually immune to contamination.

8. Relative calibration factors for certain undissociated molecules were obtained by direct calibration of the system with appropriate gas mixtures of known composition. Relative calibration factors involving dissociated species could not be obtained directly, requiring instead dependence on reported values of atomic ionization cross sections relative to molecular cross sections.

REFERENCES

1. Nagamatsu, H. T. and Sheer, R. E. "Vibrational Relaxation and Recombination of Nitrogen and Air in Hypersonic Nozzle Flows." AIAA Journal, Vol. 3, 1964, pp. 1386-1391.
2. Duffy, R. E. "Experimental Study of Nonequilibrium Expanding Flows." AIAA Journal, Vol. 3, 1965, pp. 237-244.
3. Zonars, D. "Nonequilibrium Regime of Airflows in Contoured Nozzles: Theory and Experiments." AIAA Journal, Vol. 5, 1967, pp. 57-63.
4. Muntz, E. P. "Measurement of Rotational Temperature, Vibrational Temperature, and Molecular Concentration in Non-Radiating Flows of Low Density Nitrogen." University of Toronto Institute Aerophysics Report No. 71 (AFOSR-TN-60-499), April 1961.
5. Sebacher, D. I. and Duckett, R. J. "A Spectrographic Analysis of a 1-Foot Hypersonic-Arc-Tunnel Airstream Using an Electron Beam Probe." NASA TR-R-214, December 1964.
6. Petrie, S. L., Pierce, G. A., and Fishburne, E. S. "Analysis of the Thermo-Chemical State of an Expanded Air Plasma." USAF FDL-TR-64-191, August 1965.
7. MacDermott, W. N. and Marshall, J. C. "Nonequilibrium Nozzle Expansions of Partially Dissociated Air: A Comparison of Theory and Electron-Beam Measurements." AEDC-TR-69-66 (AD690493), July 1969.
8. Hurle, I. R., Russo, A. L., and Hall, J. G. "Spectroscopic Studies of Vibrational Nonequilibrium in Supersonic Nozzle Flows." USAF ARL-65-6, January 1965.
9. Sebacher, D. I. "A Correlation of N_2 Vibrational—Translational Relaxation Times." AIAA Journal, Technical Note, Vol. 5, No. 4, April 1967, pp. 819-820.

10. Russo, A. L. "Spectrophotometric Measurements of the Vibrational Relaxation of CO in Shock Wave and Nozzle Expansion-Flow Environments." Cornell Aeronautical Laboratory, Report No. AD-1689-A-8, July 1967.

11. Bartz, J. A. and Vidal, R. J. "Research on Surface Catalysis in Nonequilibrium Flows." AEDC-TR-70-111 (AD704814), April 1970.

12. Bradley, J. N. and Kistiakowsky, G. B. "Shock Wave Studies by Mass Spectrometry. I. Thermal Decomposition of Nitrous Oxide." Journal of Chemical Physics, Vol. 35, No. 1, July 1961.

13. Carrigan, et al. "Experimental Studies to Determine the Chemical Species Prevalent in the Plasma of an Air Arc and the Boundary Layers Adjacent to Ablating Materials." WADD TR-60-359 (AD262634), October 1960.

14. O'Halloran, et al. "Determination of Chemical Species Prevalent in a Plasma Jet." ASD-TDR-62-644, Part I (AD600996), April 1964.

15. Dix, R. E. "Sampling Probe for Instantaneous Mass Spectrometric Analysis of Rarefied High Enthalpy Flow." AEDC-TR-69-37 (AD686405), March 1969.

16. Goodrich, G. W. and Wiley, W. C. "Resistance Strip Magnetic Electron Multiplier." Review of Scientific Instruments, Vol. 32, No. 7, July 1961.

17. Kieffer, L. J. and Dunn, G. H. "Electron Impact Ionization Cross Section Data for Atoms, Atomic Ions, and Diatomic Molecules: I. Experimental Data." Review of Modern Physics, Vol. 38, No. 1, January 1966.

18. Harris, C. J. and Warren, W. R. "Correlation of Nonequilibrium Chemical Properties of Expanding Air Flows." General Electric MSD R64SD92 (AD621857), December 1964.

19. Reis, V. and Fenn, J. B. "Separation of Gas Mixtures in Supersonic Jets." Journal of Chemical Physics, Vol. 39, 1963.

20. Gavril, B. D. "Generalized One-Dimensional Chemically Reacting Flows with Molecular Vibrational Relaxation." General Applied Science Laboratories, Inc., TR 426 (AD435623), January 1964.

21. Steiger, M. H. "On the Chemistry of Air at High Temperatures." General Applied Science Laboratories, Inc., Report No. TR-357, January 1963.

22. Lordi, J. A. and Mates, R. E. "Nonequilibrium Expansions of High Enthalpy Airflows." USAF Aerospace Research Laboratories, ARL 64-206, November 1964.

23. Bortner, M. H. "A Review of Rate Constants of Selected Reactions of Interest in Re-Entry Flow Fields in the Atmosphere." NBS Technical Note 484, May 1969.

24. Wilson, Jack. "A Shock-Tube Measurement of the Recombination Rate of Oxygen." (AD276626), Cornell University, Ithaca, New York, 1962.

APPENDIX
ILLUSTRATIONS

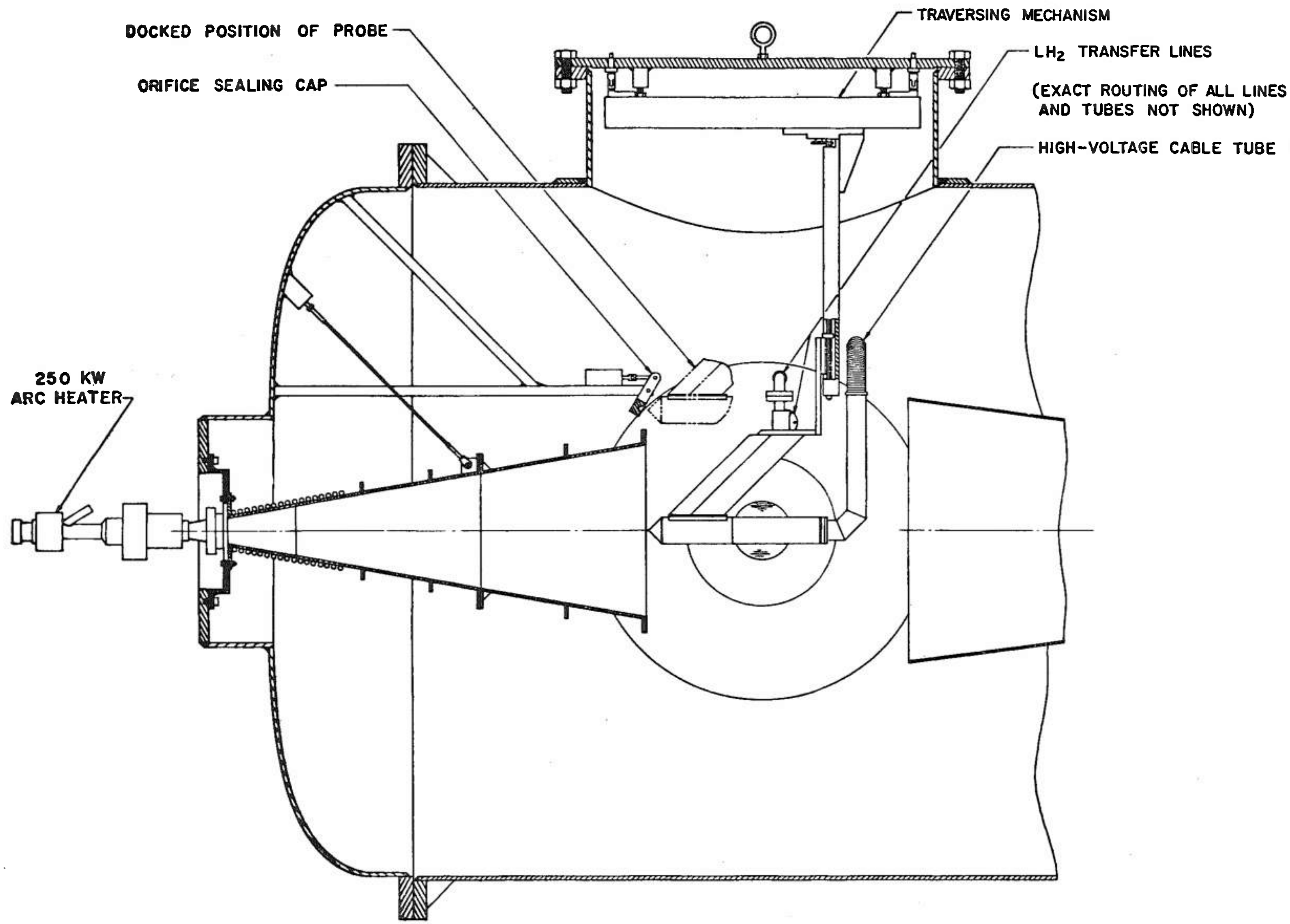

Fig. 1 The 18-in. Low-Density Wind Tunnel

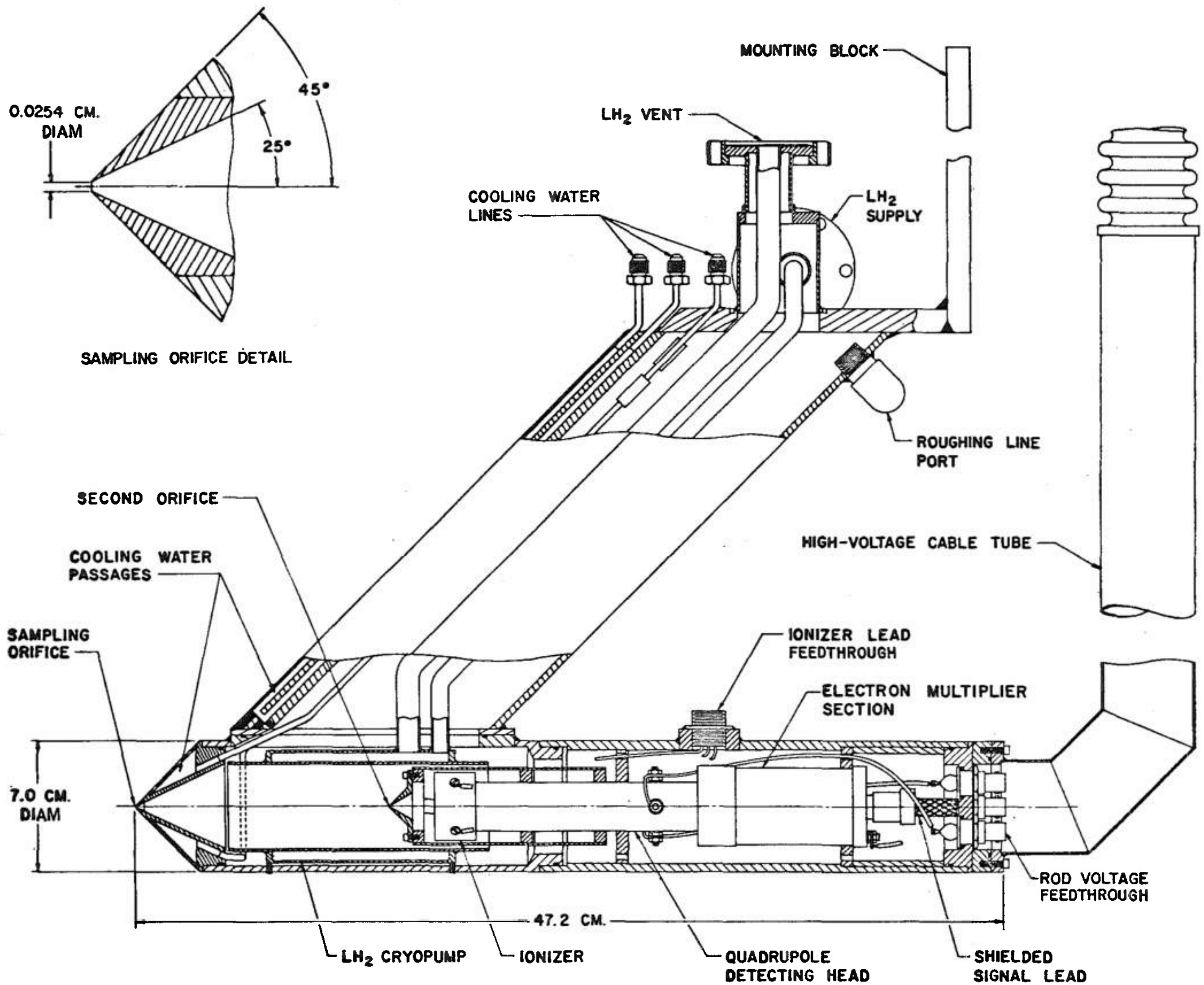

Fig. 2 Cross Section of the Mass Spectrometer Probe

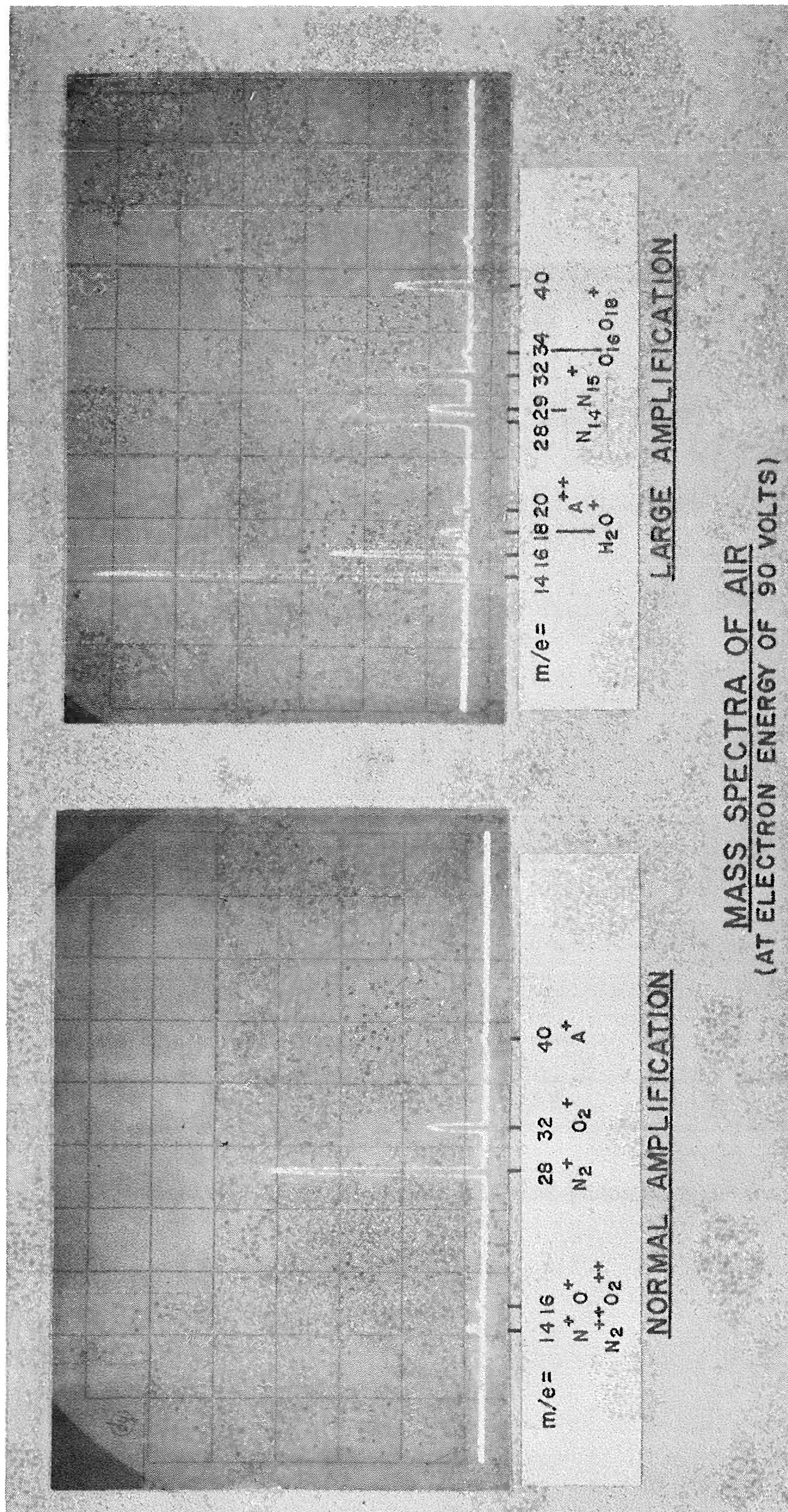

Fig. 3 Mass Spectra of Low Temperature Air

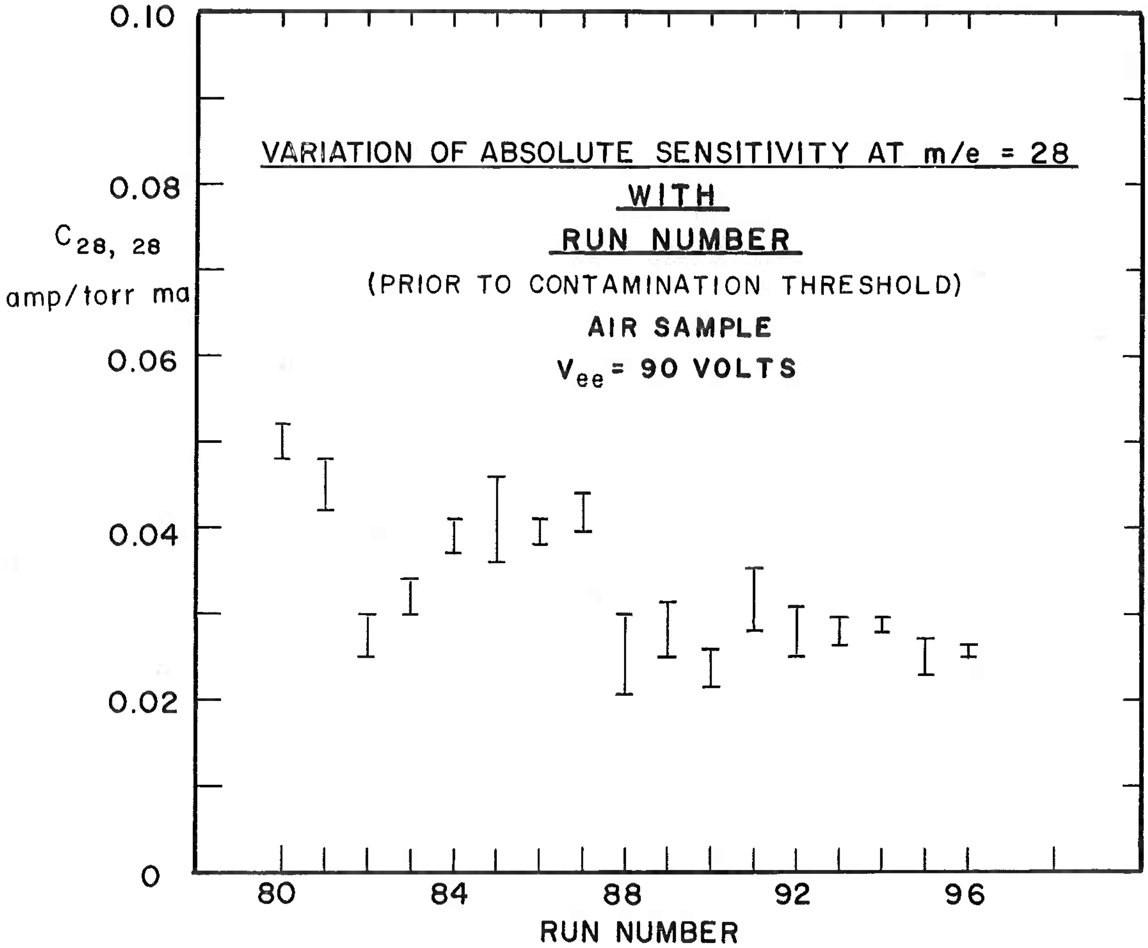

Fig. 4 Absolute Sensitivity, m/e = 28, versus Run Number

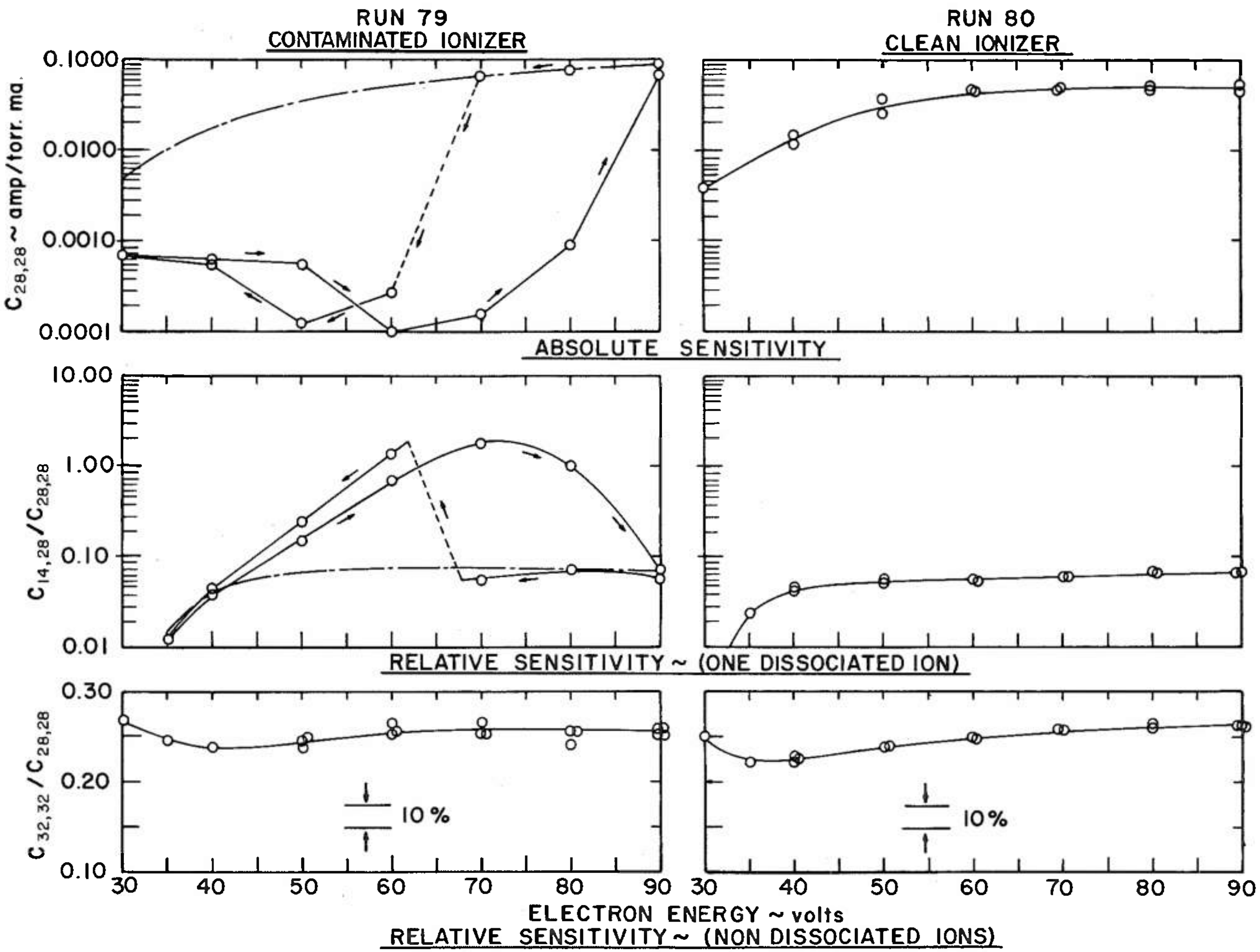

a. Contaminated Ionizer

b. Clean Ionizer

Fig. 5 Absolute and Relative Sensitivities versus Electron Energy

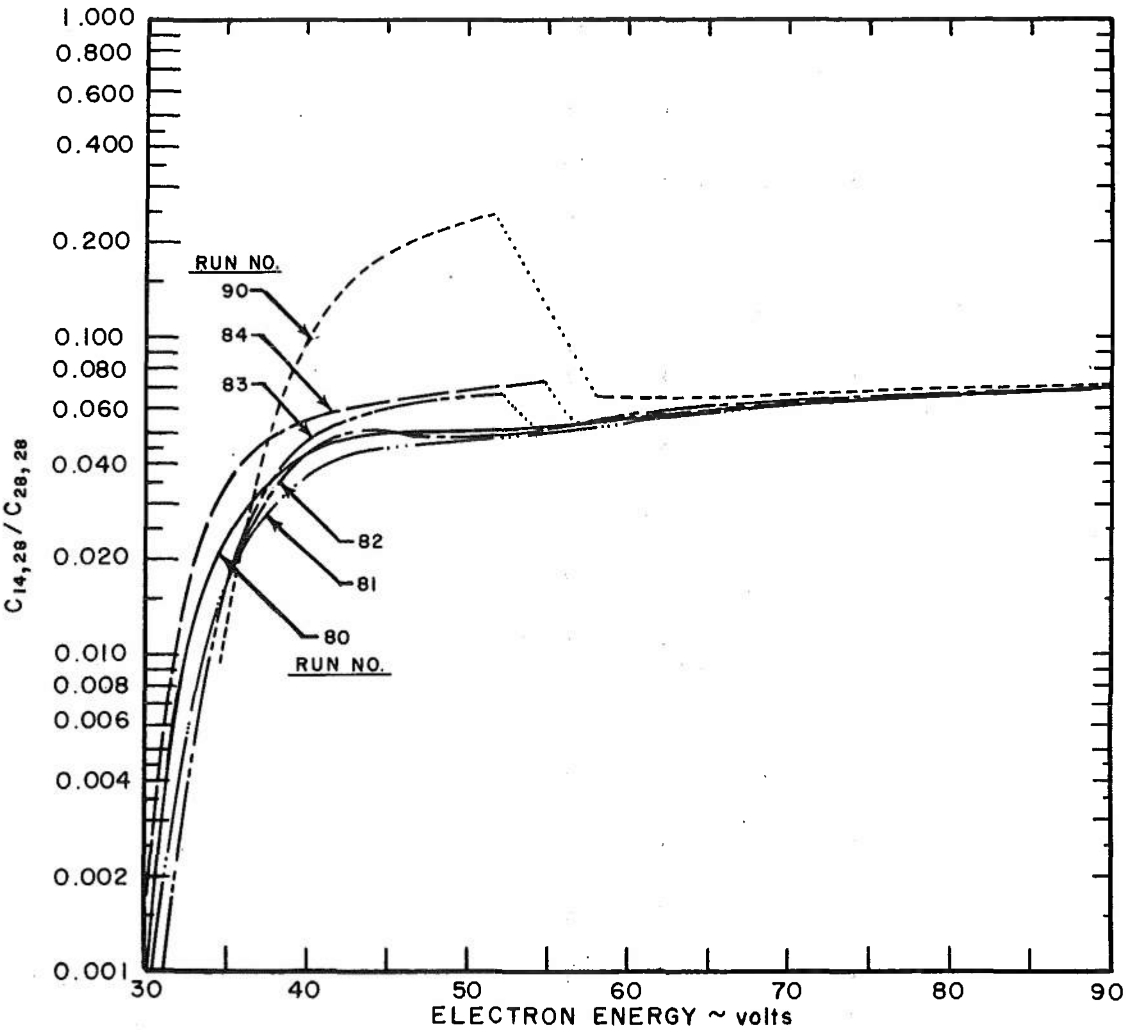

Fig. 6 Effect of Progressive Ionizer Contamination

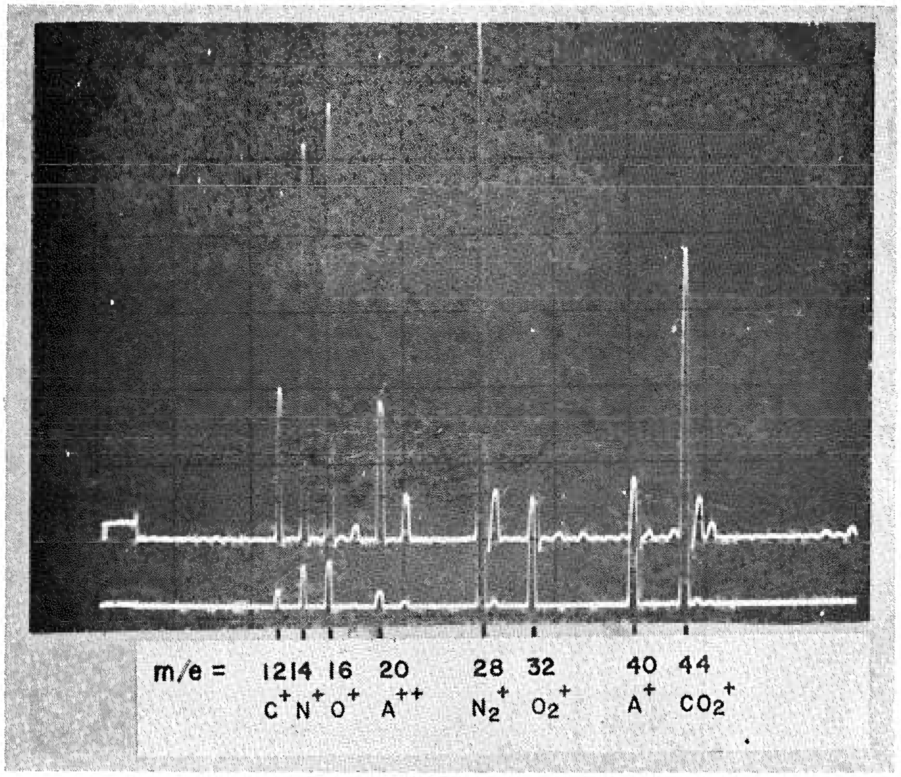

Fig. 7 Mass Spectrum for Analysis of 4-Component Mixture

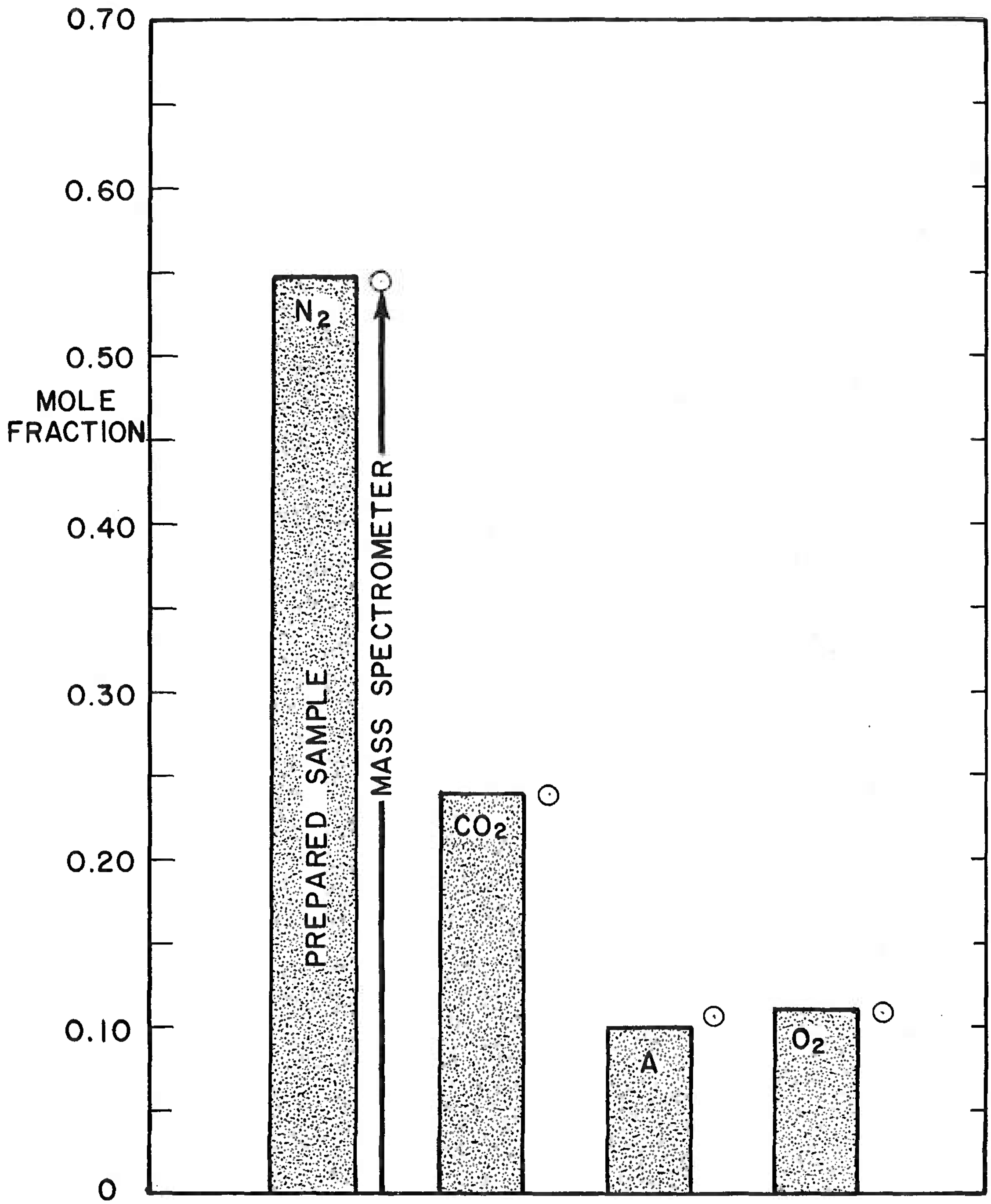

Fig. 8 Comparison of Actual and Inferred Composition of 4-Component Sample

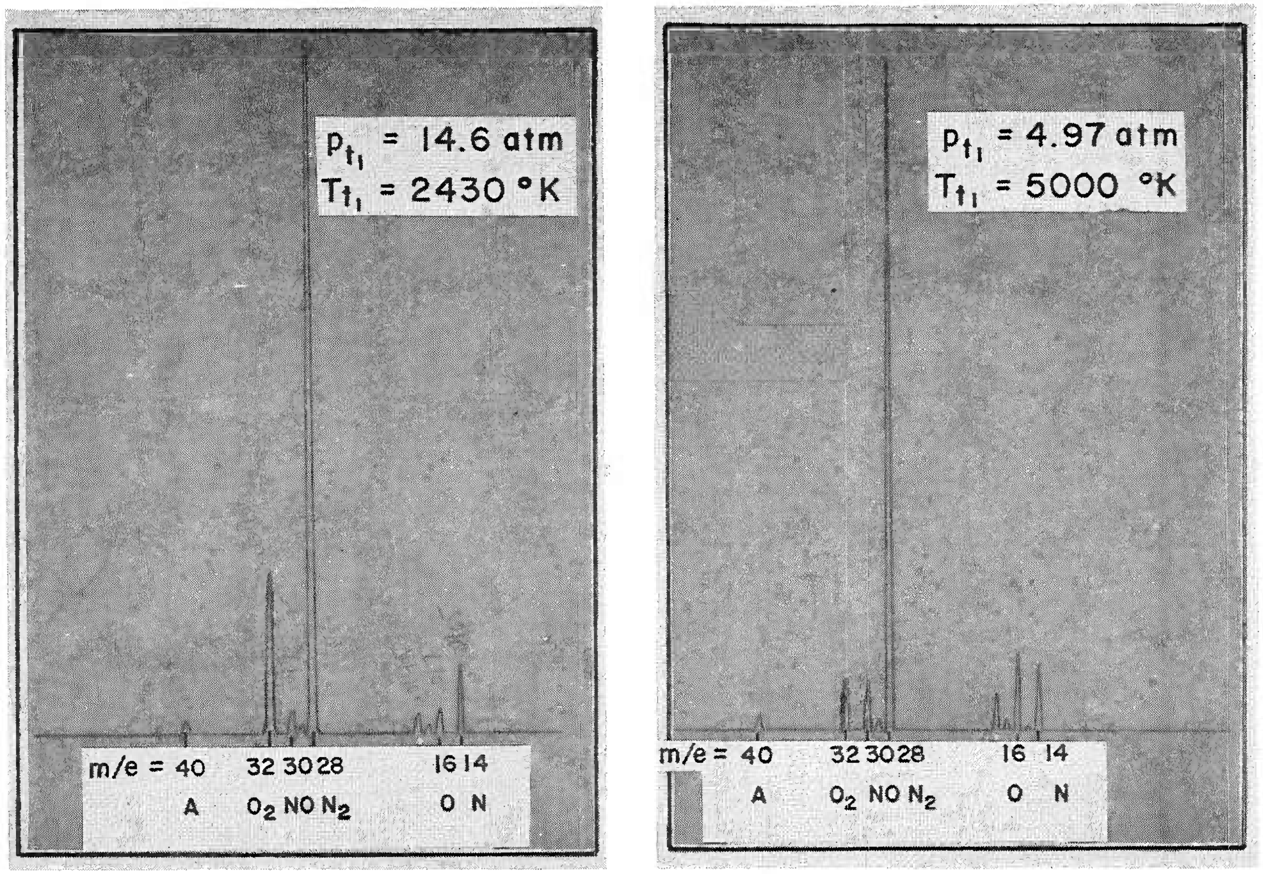

Fig. 9 Mass Spectra Obtained in Wind Tunnel

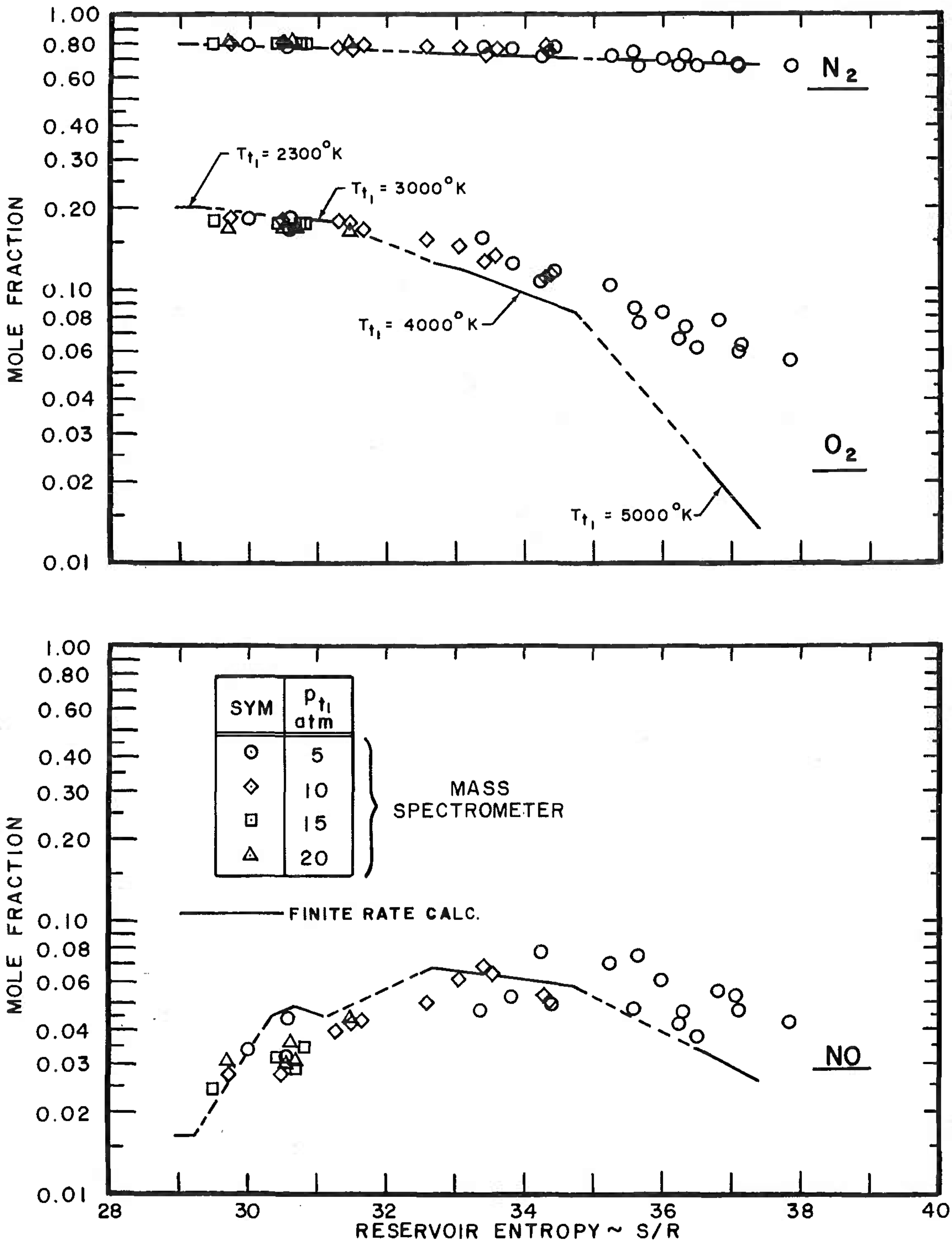

a. Molecular Species

Fig. 10 Comparison of Experimental and Theoretical Compositions in 18-in. Wind Tunnel

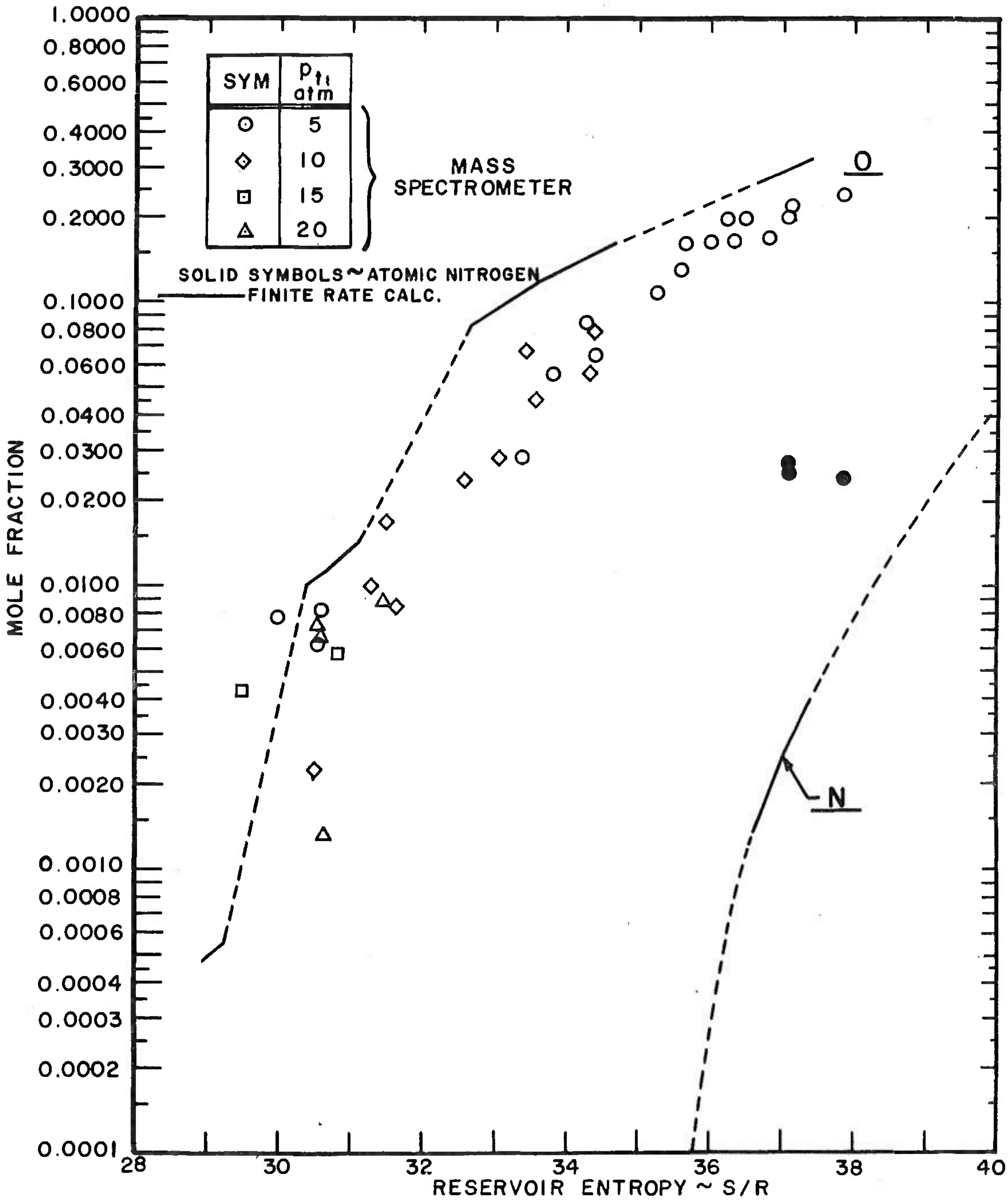

b. Atomic Species
Fig. 10 Concluded

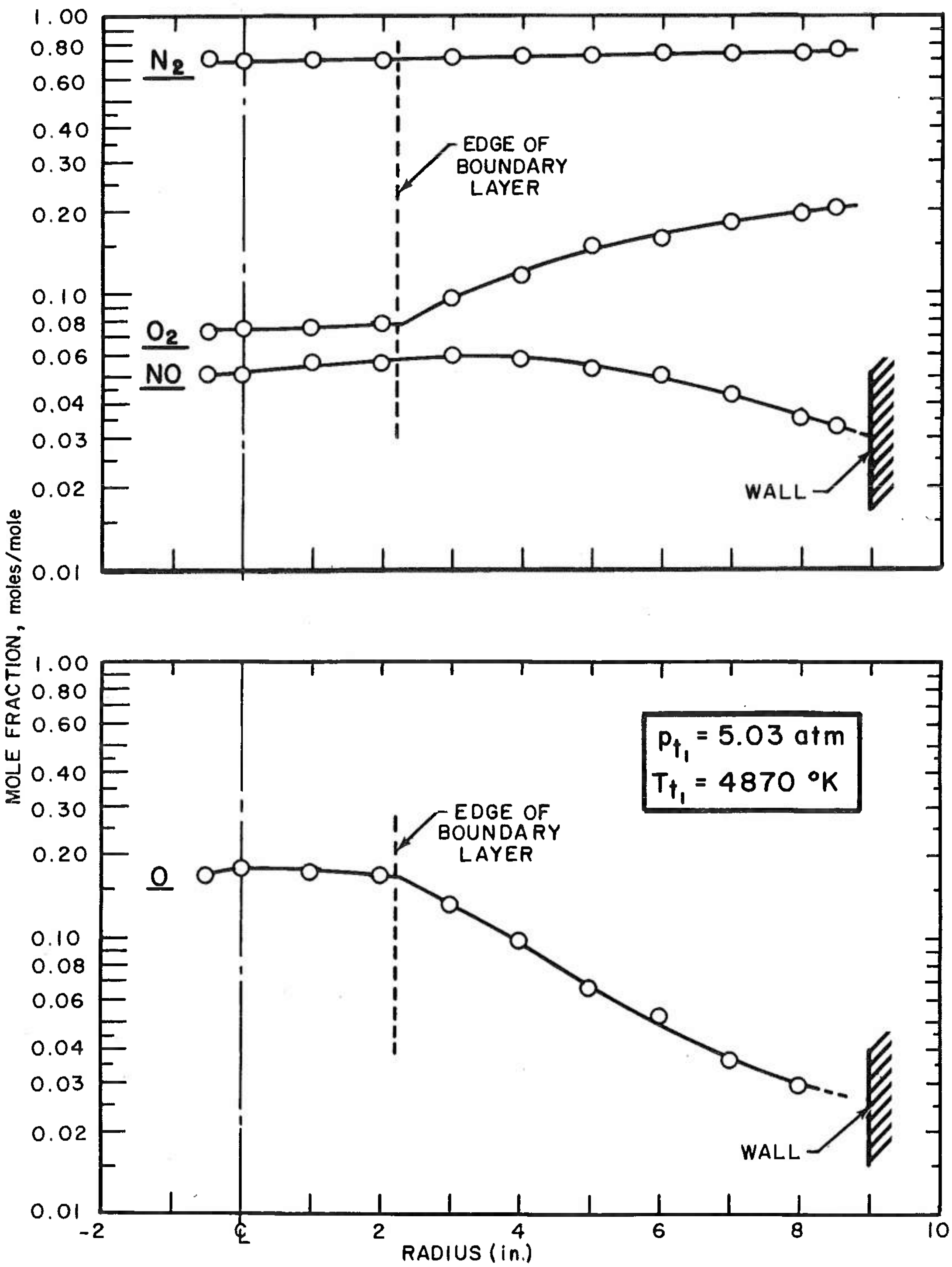

Fig. 11 Boundary Layer Composition

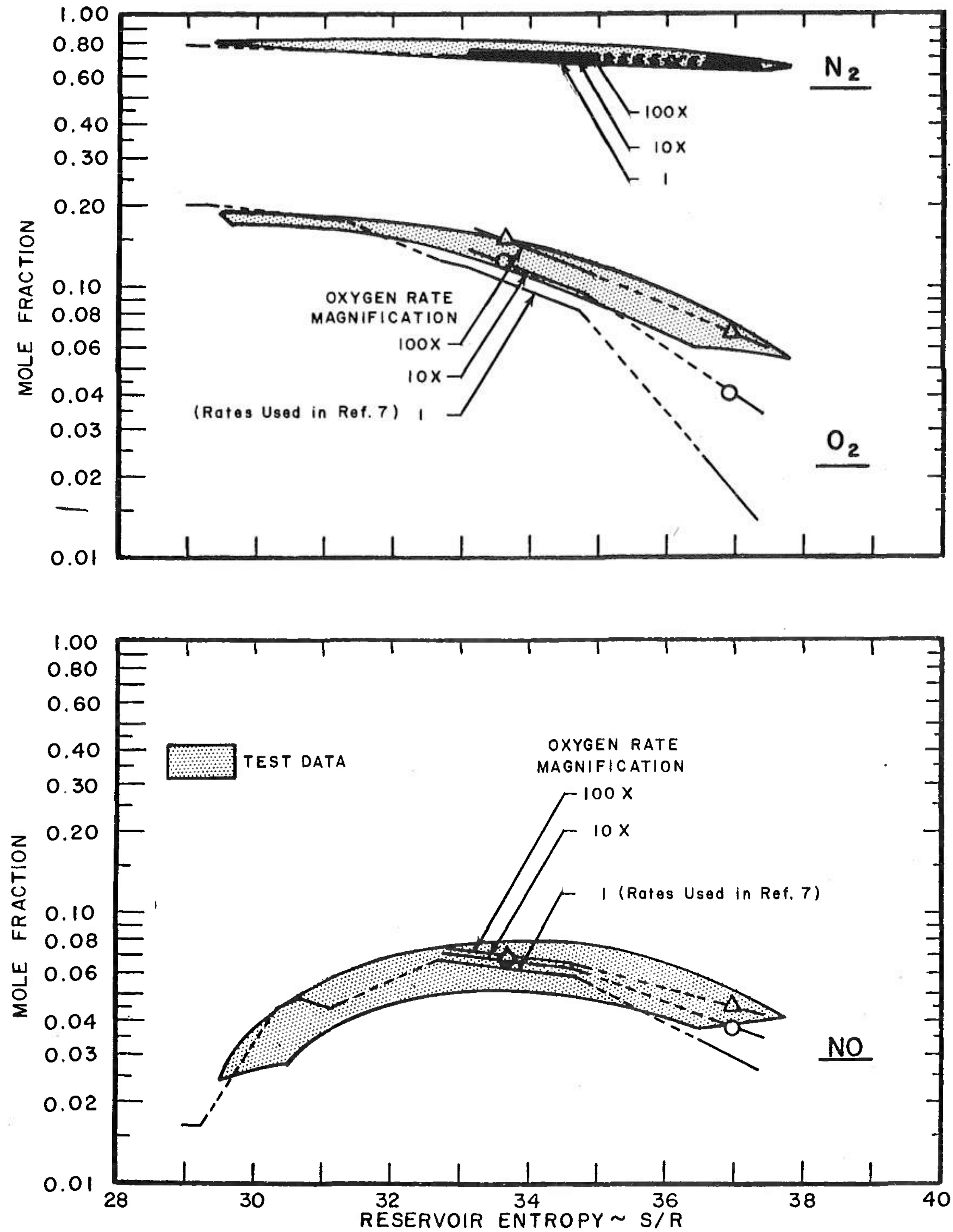

a. Molecular Species

Fig. 12 Effect of Increased Oxygen Reaction Rates on Comparison of Experimental and Theoretical Compositions

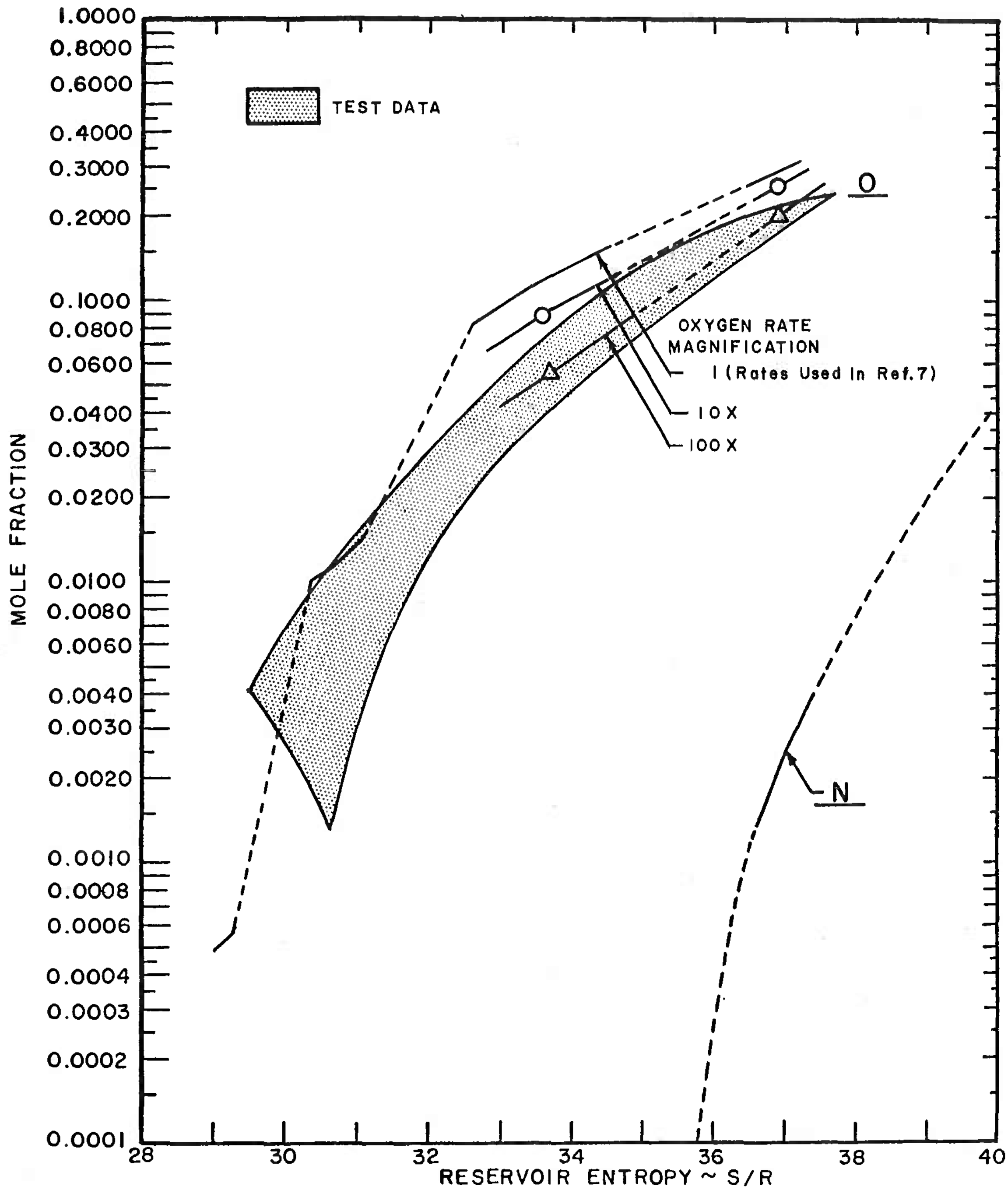

b. Atomic Species
Fig. 12 Concluded

UNCLASSIFIED

Security Classification

DOCUMENT CONTROL DATA - R & D

(Security classification of title, body of abstract and indexing annotation must be entered when the overall report is classified)

1. ORIGINATING ACTIVITY *(Corporate author)* Arnold Engineering Development Center, ARO, Inc., Operating Contractor, Arnold Air Force Station, Tennessee 37389	2a. REPORT SECURITY CLASSIFICATION UNCLASSIFIED 2b. GROUP N/A

3. REPORT TITLE

FINAL RESULTS OF ON-LINE MASS SPECTROMETRIC ANALYSIS OF EQUILIBRIUM AIRFLOWS

4. DESCRIPTIVE NOTES *(Type of report and inclusive dates)*
July 1, 1969--June 30, 1970--Final Report

5. AUTHOR(S) *(First name, middle initial, last name)*

W. N. MacDermott and R. E. Dix, ARO, Inc.

6. REPORT DATE	7a. TOTAL NO. OF PAGES	7b. NO. OF REFS
February 1971	51	24

8a. CONTRACT OR GRANT NO. F40600-71-C-0002	9a. ORIGINATOR'S REPORT NUMBER(S) AEDC-TR-71-23
b. PROJECT NO. 4344	
c. Program Element 65701F	9b. OTHER REPORT NO(S) *(Any other numbers that may be assigned this report)* ARO-PWT-TR-70-280
d. Task 02	

10. DISTRIBUTION STATEMENT

This document has been approved for public release and sale; its distribution is unlimited.

11. SUPPLEMENTARY NOTES	12. SPONSORING MILITARY ACTIVITY
Available in DDC	Arnold Engineering Development Center (XON), Air Force Systems Command, Arnold AF Station, Tenn. 37389

13. ABSTRACT Comprehensive determinations of nonequilibrium airflow compositions were made in frozen expansions of arc-heated air in a low-density wind tunnel nozzle. Reservoir conditions included pressures of from 3.7 to 20.8 atm and temperatures of from 2120 to 5380°K. The experimentally determined compositions were correlated with the reservoir entropy. At low entropy, the concentrations of molecular species were generally in close agreement with predictions based on finite rate expansion calculations, but at high entropy, where nonequilibrium effects are large, considerable deviations from the predictions were observed. The molecular oxygen content was determined to be 7 percent greater than expected. The atomic oxygen concentration was determined to be consistently less than the theoretical prediction for all values of entropy, by as much as 9 percent of the total sample in the worst case. The experimental data were consistent, however, with theoretical predictions based on oxygen recombination rates 100 times the generally accepted values. Compositions were determined with a mass spectrometric sampling probe. The notable features of the probe included a liquid-hydrogen cryopump and a quadrupole mass spectrometer. The mass spectrometer exhibited large uncertainties when attempts were made to determine absolute concentrations, particularly in a contaminated system. For determination of relative compositions in a clean system, repeatabilities of a few percent were demonstrated.

DD FORM 1 NOV 65 1473

UNCLASSIFIED

Security Classification

14. KEY WORDS	LINK A		LINK B		LINK C	
	ROLE	WT	ROLE	WT	ROLE	WT
nonequilibrium flow						
molecular flow						
wind tunnels						
mass spectrometer						
spectrometric analysis						
sampling probes						
arc heaters						